THE JOURNAL OF IMMUNOLOGY

CD40 Ligand Preferentially Modulates Immune Response and Enhances Protection against Influenza Virus

Anwar M. Hashem, Caroline Gravel, Ze Chen, Yinglei Yi, Monika Tocchi, Bozena Jaentschke, Xingliang Fan, Changgui Li, Michael Rosu-Myles, Alexander Pereboev, Runtao He, Junzhi Wang and Xuguang Li

J Immunol published online 13 June 2014
http://www.jimmunol.org/content/early/2014/06/13/jimmunol.1300093

The Journal of Immunology is published twice each month by The American Association of Immunologists, Inc., 9650 Rockville Pike, Bethesda, MD 20814-3994.

Print ISSN: 0022-1767 Online ISSN: 1550-6606.

Published June 13, 2014, doi:10.4049/jimmunol.1300093

CD40 Ligand Preferentially Modulates Immune Response and Enhances Protection against Influenza Virus

Anwar M. Hashem,[*,†,‡] Caroline Gravel,[*] Ze Chen,[§] Yinglei Yi,[§] Monika Tocchi,[*] Bozena Jaentschke,[*] Xingliang Fan,[¶] Changgui Li,[¶] Michael Rosu-Myles,[*] Alexander Pereboev,[‖,#,,††] Runtao He,[‡‡] Junzhi Wang,[¶] and Xuguang Li[*,§§]**

CD40L, a key regulator of the immune system, was studied as both a targeting ligand and a molecular adjuvant in nucleoprotein (NP)-based host defense against influenza in mouse models with different genetic backgrounds. Adenoviral vectors secreting NP-CD40L fusion protein (denoted as rAd-SNP40L) afforded full protection of immunocompetent and immunocompromised mice ($CD40L^{-/-}$ and $CD4^{-/-}$) against lethal influenza infection. Mechanistically, rAd-SNP40L preferentially induced early and persistent B cell germinal center formation, and accelerated Ig isotype-switching and Th1-skewed, NP-specific Ab response. Moreover, it drastically augmented primary and memory NP-specific CTL activity and polyfunctional $CD8^+$ T cells. The markedly enhanced nonneutralizing Abs and CTLs significantly reduced viral burdens in the lungs of mice upon lethal virus challenge. Data generated from $CD40L^{-/-}$ and $CD4^{-/-}$ mice revealed that the protection was indeed CD40L mediated but $CD4^+$ T cell independent, demonstrating the viability of the fusion Ags in protecting immunodeficient hosts. Notably, a single dose of rAd-SNP40L completely protected mice from lethal viral challenge 4 mo after immunization, representing the first report, to our knowledge, on NP in conjunction with a molecular adjuvant inducing a robust and long-lasting memory immune response against influenza. This platform is characterized by an increased in vivo load of CD40-targeted Ag upon the secretion of the fusion protein from adenovirus-infected cells and may represent a promising strategy to enhance the breadth, durability, and potency of Ag-specific immune responses. ***The Journal of Immunology*****, 2014, 193: 000–000.**

Induction of a durable and protective adaptive immune response against pathogens is the ideal outcome of vaccination. Such a process requires a cross talk between APCs including dendritic cells (DCs), macrophages, and B cells, and naive lymphocytes in secondary lymphoid organs. APCs present Ags with MHC class I or II molecules to activate naive $CD8^+$ or $CD4^+$ T cells, respectively (1, 2). B cells, in contrast, act as both APCs and Ab-secreting cells. An important aspect of the interaction between APCs and lymphocytes is the bidirectional signals that are often conveyed by various ligand-receptor ligations. These interactions provide necessary costimulatory signals to both cell types to initiate or to regulate immune responses (2, 3).

Among the various costimulatory molecules that have been identified, CD40 and its ligand (CD40L) are two of the most important molecules. They do not only orchestrate humoral and cellular immunity, but they also regulate APCs (4–7). CD40, a member of the TNF receptor superfamily, is constitutively expressed on all APCs, activated $CD4^+$ T cells, $CD8^+$ T cells, and other cell types such as fibroblasts, endothelial cells, and epithelial cells (4–7). CD40L, a member of the TNF superfamily, is mainly expressed by activated $CD4^+$ T cells transiently as a cell-surface or secreted multimer protein (4). It is also expressed by other cell types including activated B cells, some DC subsets, platelets, and smooth muscle cells (6, 7).

Interaction between CD40 and CD40L promotes the expansion and survival of APCs, T cells, and B cells to initiate and sustain immune responses (5, 6). Specifically, during DC–$CD4^+$ T cell interaction, CD40 ligation on DCs enhances their survival, secretion of cytokines, and upregulation of costimulatory receptors such as CD54, CD58, CD80, and CD86, as well as MHC class I and II molecules, thus promoting their maturation into fully competent APCs (4). Concomitantly, it provides crucial bidirectional signals to stimulate $CD4^+$ T cells themselves and/or to license DCs to initiate direct or indirect priming of CTLs (8–10). Moreover, CD40 signaling on B cells enhances not only Ag presentation to T cells (11, 12), but also their own activation and differentiation. Specifically, it facilitates Ig production, Ig isotype switching, germinal center (GC) formation, and memory B cell maturation (4, 5).

Several groups have investigated the potential of CD40L as a molecular adjuvant by either codelivering CD40L with Ags (13–20)

*Centre for Vaccine Evaluation, Biologics and Genetic Therapies Directorate, Health Canada, Ottawa, Ontario K1A 0K9, Canada; †Department of Medical Microbiology and Parasitology, Faculty of Medicine, King Abdulaziz University, Jeddah 21589, Saudi Arabia; ‡Special Infectious Agents Unit, King Fahd Medical Research Center, King Abdulaziz University, Jeddah 21589, Saudi Arabia; §Shanghai Institute of Biological Products, Shanghai 200231, China; ¶National Institutes for the Control of Food and Drug, Beijing 10050, People's Republic of China; ‖Division of Human Gene Therapy, Department of Medicine, University of Alabama at Birmingham, Birmingham, AL 35294; #Department of Obstetrics and Gynecology, University of Alabama at Birmingham, Birmingham, AL 35294; **Department of Pathology and Surgery, University of Alabama at Birmingham, Birmingham, AL 35294; ††Gene Therapy Center, University of Alabama at Birmingham, Birmingham, AL 35294; ‡‡National Microbiology Laboratory, Public Health Agency of Canada, Winnipeg, Manitoba R3E 3R2, Canada; and §§Department of Biochemistry, Microbiology and Immunology, University of Ottawa, Ottawa, Ontario K1H 8M5, Canada

Received for publication January 15, 2013. Accepted for publication May 8, 2014.

This work was supported by the King Abdulaziz University (A.M.H.) and the Canadian Regulatory Strategy for Biotechnology.

Address correspondence and reprint requests to Prof. Xuguang Li or Dr. Junzhi Wang, Centre for Vaccine Evaluation, Biologics and Genetic Therapies Directorate, Health Canada, Ottawa, ON K1A OK9, Canada (X.L.) or National Institutes for Food and Drug Control, No. 2, Tiantan Xili, Beijing 100050, China (J.W.). E-mail addresses: Sean.Li@hc-sc.gc.ca (X.L.) or wangjz@nicpbp.org.cn (J.W.)

The online version of this article contains supplemental material.

Abbreviations used in this article: DC, dendritic cell; F, trimerization motif from the T4 bacteriophage fibritin; GC, germinal center; HA, hemagglutinin; LN, lymph node; NA, neuraminidase; NP, nucleoprotein; rAd, recombinant adenovirus; S, secretion signal peptide.

or retargeting the Ag-delivery vector to CD40 on APCs (21–30). Although enhanced immune responses against various pathogens and tumors were observed, little is known about in vivo B cell responses, functional roles of $CD4^+$ and $CD8^+$ T cells during induction phase, or the contributions of Abs and $CD8^+$ T cells in protection.

Influenza is a highly contagious virus that causes respiratory tract infection, which represents a serious burden to public health. Current influenza vaccines largely induce strain-specific neutralizing Abs against the two surface glycoproteins: hemagglutinin (HA) and neuraminidase (NA). However, the high antigenic variability of both HA and NA necessitates annual vaccine formulation and evaluation, reviewed by Hashem et al. (31). In contrast, internal proteins such as nucleoprotein (NP) are highly conserved among all influenza A subtypes but proven to elicit limited protection in animals (32–37). Although CD40L was found to enhance immune response against the highly variable HA protein (26, 30), only partial protection was obtained even with multiple-dose immunizations.

In this article, we determined the potential of CD40L as both an Ag-targeting ligand and a molecular adjuvant to enhance NP-induced host defense against influenza. Our results clearly show that targeting influenza NP via CD40L resulted in $CD4^+$ T cell–independent/$CD8^+$ T cell–dependent protection that involved both B cell and $CD8^+$ T cell activation. This enhanced protection was predominantly dependent on targeting NP to CD40-expressing cells via CD40L. Notably, we show for the first time, to our knowledge, that a single dose of recombinant adenovirus (rAd) encoding secreted NP-CD40L (SNP-CD40L) fusion protein can induce robust and long-lasting protective memory immune response against influenza.

Materials and Methods

Cell lines and influenza virus

NIH-3T3 (ATCC: CRL-1658), MDCK (ATCC: CCL-34), and QBI-HEK 293A cells were cultured as described previously (38). Mouse-adapted influenza A/Puerto Rico/8/34(H1N1) and A/Jingke/30/95(H3N2) viruses were used for viral challenge.

Generation of rAds

Constructs were designed to express influenza A/duck/Yokohama/aq10/03 (H5N1) NP (GenBank accession no. AB212281, http://www.ncbi.nlm.nih.gov/genbank) intracellularly (rAd-NP), a secreted form of NP (rAd-SNP) consisting of influenza NP and 23 aa (MLLAVLYCLLWSFQTSAGHFPRA) from the human tyrosinase signal peptide (GenBank accession no. AH003020, http://www.ncbi.nlm.nih.gov/genbank) at the N terminus as previously described (39), a fusion protein expressed by rAd-SNP40L consisting of SNP followed by a 27-aa fragment from the bacteriophage T4 fibritin trimerization motif (GYIPEAPRDGQAYVRKDGEWVLLSTFL) connected to the ectodomain of mouse CD40L (GenBank accession no. NM_011616, http://www.ncbi.nlm.nih.gov/genbank; aa 117–260) as previously described (22), unsecreted CD40-targeted fusion protein (rAd-NP40L) or an empty control vector (rAd-Control). rAds were generated using AdenoVator Adenoviral Expression System with pAdenoVator-CMV5 (Cuo)-IRES-GFP transfer vector (tAd; Qbiogene, Carlsbad, CA) according to the manufacturer's instructions and as previously described (37).

In brief, coding sequences for influenza A/duck/Yokohama/aq10/03 (H5N1) NP and mouse CD40L were synthesized by Bio S&T (Montreal, QC, Canada) in pUC19 vector (pNP and pCD40L, respectively). All PCRs were done using High Fidelity Iproof kits (Bio-Rad Laboratories, Mississauga, ON, Canada). Primers used are listed in Supplemental Table I. All genes were cloned between NotI and EcoRV sites in the tAd vector. For tAd-NP, NP was PCR amplified from pNP with NP-1 and NP-R1 primers to introduce NotI and EcoRV sites, respectively. NP gene was PCR amplified from pNP introducing 43 bp of the secretion signal peptide (S) at the 5′ terminus and EcoRV site at the 3′ end using NP-2 and NP-R1 primers, to generate tAd-SNP. PCR product was reamplified to complete the secretion sequence to 69 bp introducing NotI site at the 5′ end using NP-3 and NP-R1 primers. The tAd-SNP40L was assembled in three steps. First, SNP fusion gene was PCR amplified from tAd-SNP using NP-3 and NP-R2 to introduce 41 bp of the trimerization motif from the T4 bacteriophage fibritin (F) at the 3′ terminus, which contains an internal HindIII restriction site, and to generate SNPΔF. Second, the ectodomain of CD40L (nt 361–795) was PCR amplified in a separate reaction from pCD40L using CD40L-1 and CD40L-R primers to add 27 bp from the F at the 5′ end and EcoRV site at the 3′ end, respectively. PCR product was reamplified to add 29 bp of the trimerization motif, which contains the internal HindIII restriction site, using CD40L-2 and CD40L-R primers, and to generate ΔFCD40L. Finally, both fragments, SNPΔF and ΔFCD40L, were gel purified, digested with HindIII, ligated, and PCR amplified using NP-3 and CD40L-R primers. SNPFCD40L fragment was digested and inserted into the tAd vector. Fusion gene was amplified from tAd-SNP40L using NP-1 and CD40L-R primers, and inserted into the tAd vector, to generate tAd-NP40L. Cloning was confirmed by DNA sequencing and restriction enzyme digestion. rAds were then generated, purified, and titrated as previously described (37).

Protein expression and secretion in cell culture

Generated rAds were used to infect confluent NIH-3T3 cells in six-well plates at a multiplicity of infection of 100. Forty-eight hours later, supernatants were collected and immunoprecipitated with polyclonal anti-NP Abs using either protein G agarose beads or Pierce Crosslink Magnetic IP/Co-IP Kits (Pierce Biotechnology, Rockford, IL) according to the manufacturer's instructions. Cells were also washed with PBS and lysed using SDS-lysis buffer containing 20 mM Tris, pH 7.5, 150 mM NaCl, 0.5% SDS, 0.5% Tergitol-type NP-40, 0.5% deoxycholate, 1 mM EDTA, and Complete Mini PMSF protease inhibitors (Roche, Indianapolis, IN). Protein expression and secretion were confirmed by Western blot as described previously (40) using rabbit polyclonal anti-NP Abs.

Animal studies

Six- to 8-wk-old female BALB/c mice were purchased from Charles River Laboratories (Wilmington, MA). Eight- to 10-wk-old female C57BL/6J, B6.129S2-*Cd4*^{tm1Mak}/J (CD4 deficient; $CD4^{-/-}$), B6.129S2-*Cd8a*^{tm1Mak}/J (CD8 deficient; $CD8^{-/-}$), and B6.129S2-*Cd40lg*^{tm1Imx}/J (CD40L deficient; $CD40L^{-/-}$) mice were purchased from Jackson Laboratories (Bar Harbor, ME). All animal experiments were conducted in accordance with Health Canada institutional guidelines and the approval of the Animal Care and Use Committee.

The immunization dose was 1×10^9 PFU of each rAd virus. Blood samples or cells from spleens and/or draining lymph nodes (LNs) were collected as described previously (23). BALB/c and C57BL/6J mice were intranasally challenged with $10\times$ LD_{50} of either influenza A/Puerto Rico/8/34(H1N1) or A/Jingke/30/95(H3N2) viruses, whereas $CD40L^{-/-}$, $CD4^{-/-}$, and $CD8^{-/-}$ mice were challenged with $5\times$ LD_{50} of influenza A/Puerto Rico/8/34(H1N1) virus at time points indicated in the figure legends. Survival rates are presented as a percentage of surviving animals at each time point compared with the initial number of animals in each group. Weight loss is expressed as percentage of animal weight at each time point from their initial body weight. Clinical scoring was performed according to the following grading scale: healthy, 0; barely ruffled fur, 1; ruffled fur but active, 2; ruffled fur and inactive, 3; ruffled fur, inactive and hunched, 4; dead, 5, as described previously (41).

ELISA

The end-point titer of each anti-NP Ab isotypes (IgG1, IgG2a, IgG2b, IgG2c, or IgM) from immunized mice was determined by ELISA as described previously (37) with minor modifications. In brief, 96-well plates coated with purified rNP protein were blocked with 5% nonfat dry milk in PBS containing 0.05% Tween 20 for 1 h at 37°C. Then 100 μl/well of each serum sample from immunized mice at the indicated time points was added in a 2-fold serial dilution starting from 1:100 or 1:1000 dilution in blocking buffer and incubated at 37°C for 1 h. After washing, appropriate HRP-conjugated rabbit anti-mouse Abs, anti-IgG1, anti-IgG2a, anti-IgG2b, anti-IgG2c, or anti-IgM (Jackson Immunoresearch Laboratories West Grove, PA), were added at 1:2000 dilution in blocking buffer for 1 h at 37°C. IgG2a was detected in BALB/c mice, whereas IgG2c isotype was detected in C57BL/6J; we refer to IgG2c as IgG2a/c as previously described (42). Tetramethylbenzidine substrate (Cell Signaling Technology, Danvers, MA) was added for 30 min at room temperature for colorimetric development, and the reaction was stopped with 0.16 M sulfuric acid. Absorbance was read spectrophotometrically at 450 nm. End-point Ab titers were expressed as the reciprocals of the final detectable dilution with a cutoff defined as the mean of prebleed samples plus 3 SD.

$CD8^+$ T cell intracellular cytokine staining

Primary and memory $CD8^+$ T cell IFN-γ, TNF-α, and IL-2 responses were evaluated at 4 wk after primary and secondary immunizations as previ-

ously described (37) in BALB/c mice. In brief, splenocytes (1×10^6) were cultured in RPMI 1640 medium with 10% FBS in the presence of 5 μg/ml synthetic NP MHC class I–restricted peptide (TYQRTRALV) (restricted to H-2Kd) for ex vivo restimulation and 1 μg/ml GolgiPlug for 6 h. Stimulated cells were stained with allophycocyanin-eFluor 780–conjugated anti-mouse CD8a (clone 53-6.7; eBiosciences), PerCP-Cy5.5–conjugated anti-mouse IFN-γ (clone XMG1.2; eBiosciences); PE-conjugated anti-mouse TNF-α (clone MP6-XT22; eBiosciences), and Pe-Cy7–conjugated anti-mouse IL-2 (clone JES6-5H4; eBiosciences). Results for IFN-γ, TNF-α, and IL-2 were calculated as a percentage of $CD8^+$ T cells.

Polyfunctional $CD8^+$ T cells were analyzed using Boolean gate analysis as described previously (43). A BD LSRII flow cytometer was used for data acquisition, and analysis was completed with Flow Jo, Version 8.8.4 (Tree Star, Ashland, OR). Unstained cells and single-stained compensation beads (BD Biosciences, Mississauga, ON) were used as controls for background fluorescence and false-positives because of fluorochrome bleeding.

CTL assay

CTL assay was conducted using lactate dehydrogenase release assay as previously described (37). In brief, 3×10^7 splenocytes from immunized BALB/c mice were restimulated in vitro to generate effector CTLs. After 5 d of culture, cytotoxic activity was measured by lactate dehydrogenase release using NP peptide-pulsed P815 targets (H-2d). The percentage of specific lysis was calculated as (experimental release − effector spontaneous release − target spontaneous release)/(maximum release − target spontaneous release) × 100%.

B cell flow cytometry

Single-cell suspensions of LNs or spleens from immunized BALB/c mice were washed twice with FACS buffer (PBS with 5% FBS) and stained with Pe-Cy7–conjugated anti-mouse CD19 (clone 1D3; eBiosciences), allophycocyanin-eFluor780–conjugated anti-mouse CD45R/B220 (clone RA3-6B2; eBiosciences), PerCP-conjugated anti-mouse IgG (Jackson Immunoresearch), allophycocyanin-conjugated anti-mouse IgD (clone 11-26; eBiosciences), Alexa Flour 488–conjugated anti-mouse Ly77/GL7 (clone GL-7; eBiosciences), and PE-conjugated anti-mouse Syndecan-1/CD138 (clone 281-2; BD Biosciences) for 30 min at 4°C. In another experiment, cells were stained with PE-conjugated anti-mouse CD19 (clone 1D3; eBiosciences), FITC-conjugated anti-mouse B7.1/CD80 (clone 16-10A1; eBiosciences), and Pe-Cy5–conjugated anti-mouse CD40 (clone 1C10; eBiosciences). Stained cell samples were fixed with 1% paraformaldehyde. A BD LSRII flow cytometer was used for data acquisition, and analysis was completed with FlowJo as described earlier.

$CD8^+$ T cells adoptive and serum passive transfer

$CD8^+$ T cells were purified from splenocytes obtained from immunized BALB/c mice by negative selection using the Dynal Mouse CD8 Negative Isolation Kit (Life Technologies, Burlington, ON). Purity of $CD8^+$ T cells was determined using PE-conjugated anti-mouse CD8α (clone 53-6.7; eBiosciences) and Pe-Cy7–conjugated anti-mouse CD3 (clone 145-2C11; eBiosciences), and found to be >95% pure. Naive BALB/c mice were injected i.v. via the tail vein with 1×10^7 $CD8^+$ T cells using a 27-gauge needle. Three days later, they were intranasally challenged with $10\times$ LD_{50} of influenza A/Puerto Rico/8/34(H1N1) virus. In another experiment, naive BALB/c mice were injected i.p. with 300 μl donor serum from BALB/c mice immunized with the different rAd constructs on days −3 to +1 relative to infection. On day 0, mice were intranasally challenged with $10\times$ LD_{50} of influenza A/Puerto Rico/8/34(H1N1) virus. Lungs were harvested from mice 6 d postchallenge and used for viral titration by plaque assay in MDCK cells as described previously (44). Titers were expressed as $\log_{10}$ PFU/g tissue.

Data analysis

Statistical analysis was conducted using either one-way or two-way ANOVA when appropriate. Gehan–Breslow–Wilcoxon test was used for survival curves. Bonferroni posttest was used to adjust for multiple comparisons between the different groups. All statistical analysis was conducted using GraphPad Prism software (San Diego, CA).

Results

rAd construction and in vitro protein expression and secretion

Our goal was to determine whether CD40L, as an adjuvant and targeting molecule, could enhance specific immune response against NP, a highly conserved but much less effective protective immunogen compared with the surface glycoproteins (32–34, 36, 37). We generated rAd vector expressing NP fused to an S at the N terminus and a trimerized form of murine CD40L ectodomain at the C terminus (rAd-SNP40L) (Fig. 1A). rAd-SNP40L can infect various cell types in vivo, which subsequently would secret NP-CD40L fusion protein to activate $CD40^+$ APCs. The controls include rAd encoding, a nonsecreted form of NP-CD40L (rAd-NP40L); rAd expressing nontargeting but secreted-NP (rAd-SNP); rAd-NP expressing nonsecreted NP intracellularly; and an empty vector control.

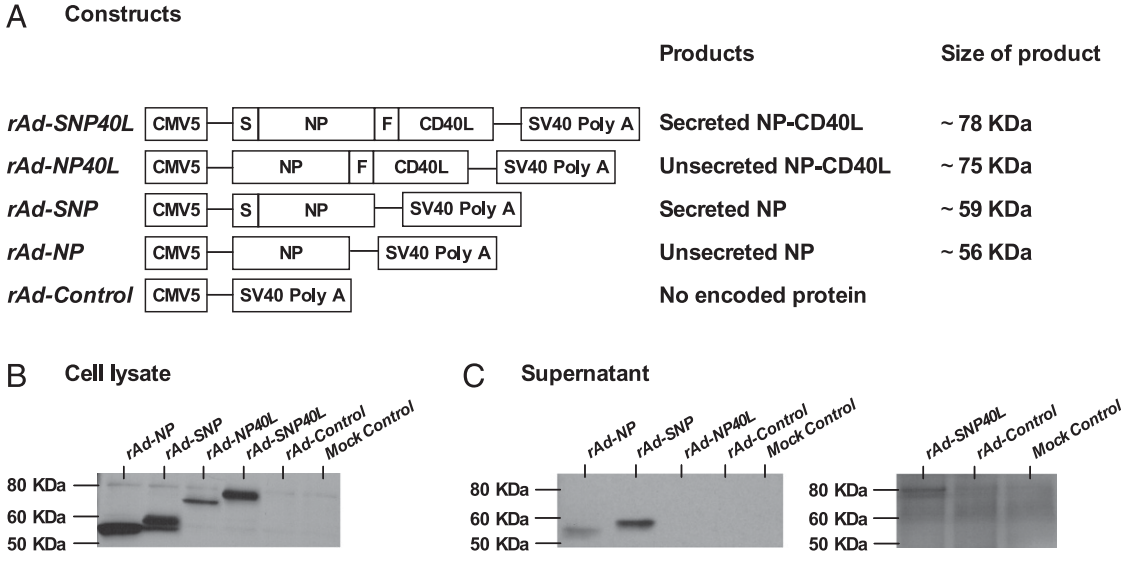

FIGURE 1. rAd constructs and in vitro protein expression and secretion. (**A**) Schematic representation of the generated rAd constructs. The rAd-SNP40L expresses secreted NP-CD40L fusion protein. The rAd-NP40L encodes the fusion protein missing the S. rAd-NP and rAd-SNP express NP and secreted NP, respectively. The rAd-Control is an "empty" control vector. Numbers indicate the expected m.w. of the proteins from each construct. (**B**) In vitro protein expression in cell lysates collected from NIH/3T3 cells 48 h postinfection with rAds at multiplicity of infection of 100. (**C**) In vitro protein secretion in cell culture supernatant collected 48 h postinfection. Protein expression and secretion were confirmed by Western blot using anti-NP Abs. F, trimerization motif from the T4 bacteriophage fibritin; NP, influenza A/duck/Yokohama/aq10/03(H5N1) NP.

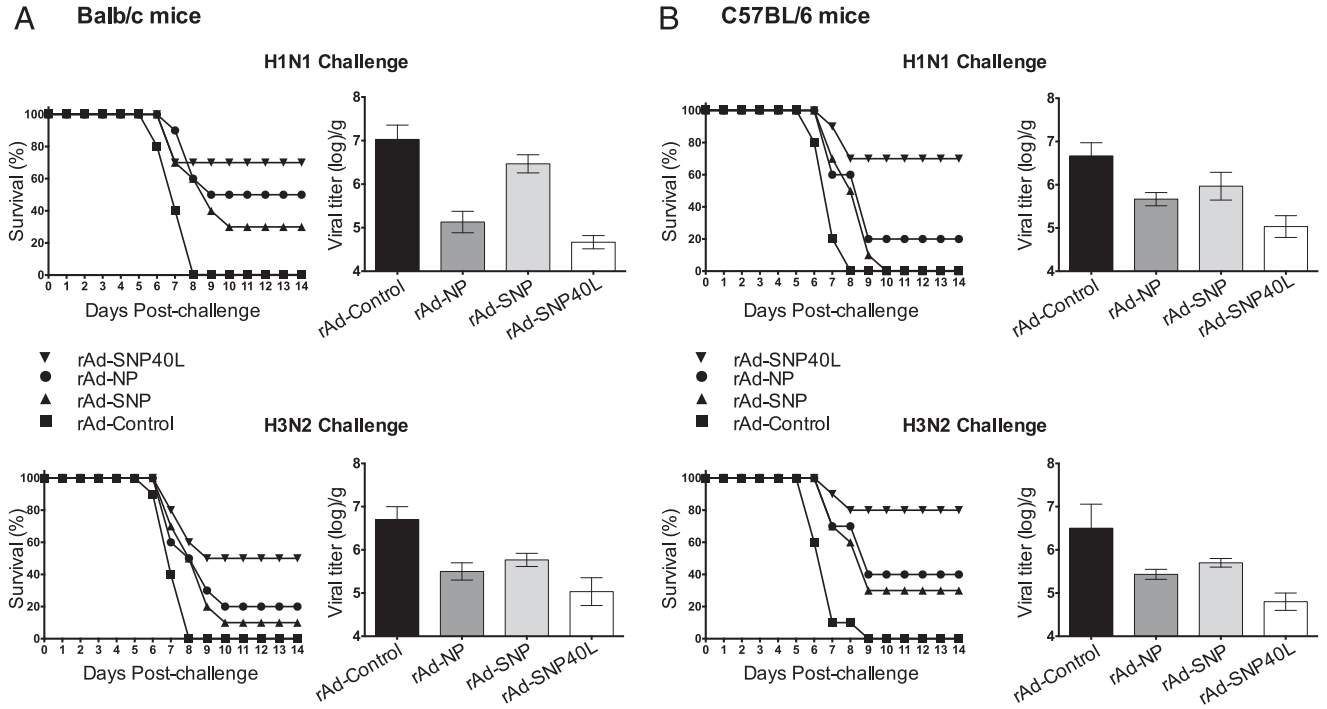

FIGURE 2. Targeting NP via CD40L provides heterosubtypic protection in wild-type BALB/c and C57BL/6J mice. Survival curves and lung viral titer of (**A**) BALB/c and (**B**) C57BL/6J mice immunized with two doses of 10^9 PFU of the indicated rAd constructs and challenged with 10× LD_{50} of mouse-adapted influenza A/Puerto Rico/8/1934(H1N1) or A/Jingke/30/95(H3N2) viruses 4 wk after secondary immunization are shown. Data are shown from one of two experiments with $n = 10$ mice per treatment group in survival curves and from one experiment with $n = 3$ mice per treatment group in lung viral titers.

Before animal immunizations, NP proteins expressed from the transgenes were confirmed. As shown in Fig. 1B, Western blot confirmed the expression of NP, SNP, NP40L, and SNP40L in cell lysates. Supernatant from infected cells was immunoprecipitated using anti-NP Abs and analyzed by Western blot, to confirm protein secretion by rAd-SNP and rAd-SNP40L (Fig. 1C). Protein secretion was confirmed from both rAd-SNP (Fig. 1C, *lane 2*) and rAd-SNP40L (Fig. 1C, *lane 6*). The detection of NP from rAd-NP

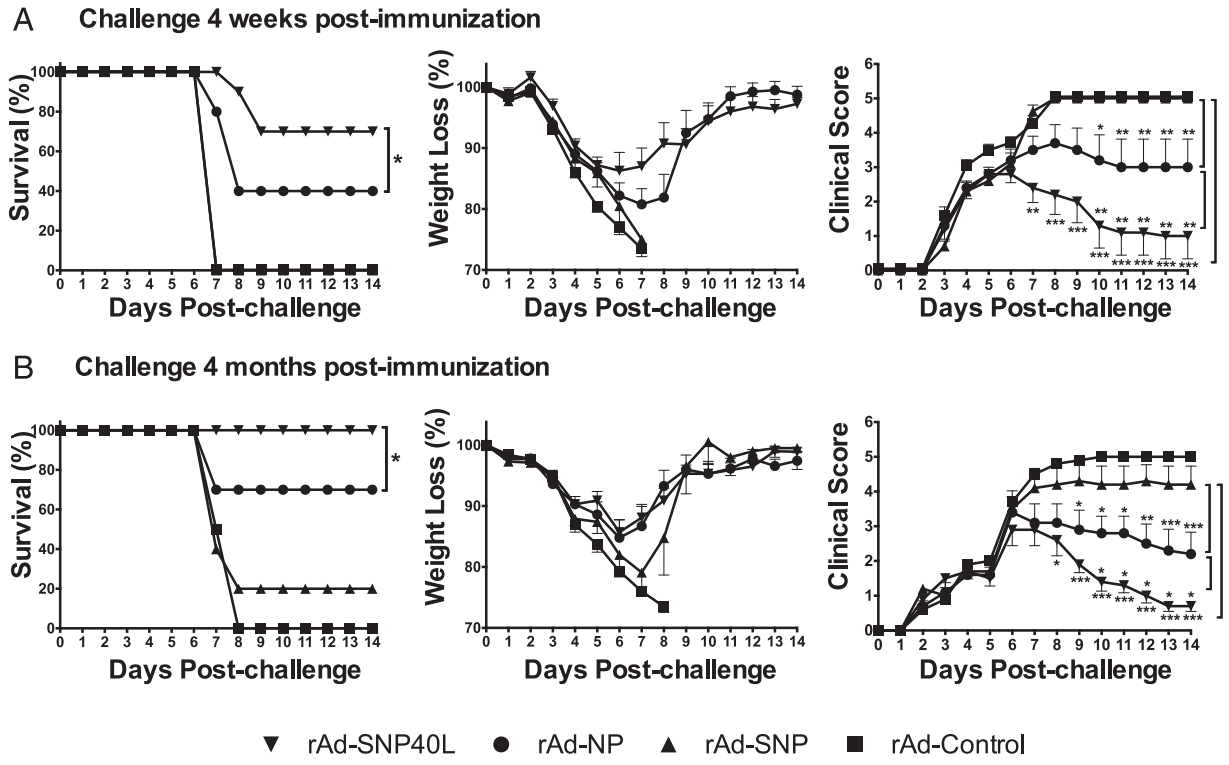

FIGURE 3. Single dose of rAd-SNP40L confers enhanced protection against influenza infection in wild-type BALB/c mice. Survival curves, body weight loss, and clinical score of BALB/c mice immunized with a single dose of the indicated rAd constructs and challenged with 10× LD_{50} of influenza A/Puerto Rico/8/34(H1N1) virus either (**A**) 4 wk or (**B**) 4 mo postimmunization. Data are shown from one of two experiments with $n = 10$ mice per treatment group. ***$p <$ 0.001, **$p < 0.01$, *$p < 0.05$ (two-way ANOVA with Bonferroni posttest for clinical score and Gehan–Breslow–Wilcoxon test for survival curves).

in supernatant (Fig. 1C, *lane 1*) was expected because small amounts of extracellular NP can be observed in cell culture supernatant (45).

Immunization with rAd-SNP40L provides heterosubtypic protection in BALB/c and C57BL/6J mice

We next evaluated the protective efficacy of these constructs in BALB/c and C57BL/6J mice against lethal H1N1 and H3N2 influenza virus challenges. Of note, initial pilot experiments showed that rAd-NP40L was unable to induce any detectable Ab response or to confer any protection in BALB/c mice; thus, this construct was excluded from all subsequent studies (see *Discussion*). Moreover, as shown in Fig. 2, immunization with two doses of rAd-SNP40L conferred enhanced protection against both viral strains in both mouse models compared with other constructs. This was accompanied by markedly reduced viral replication in the lungs of the mice immunized with rAd-SNP40L (Fig. 2).

Single dose of rAd-SNP40L provides durable protection against lethal challenge

We then evaluated the protective efficacy of a single dose of these constructs in BALB/c mice against a lethal challenge. When immunized mice were challenged with H1N1 influenza strain 4 wk after a single immunization with either rAd-SNP40L or rAd-NP, 14-d survival rates were 70 and 40%, respectively (Fig. 3A). Furthermore, rAd-SNP40L–immunized BALB/c mice were completely protected against H1N1 influenza strain when challenged 4 mo postimmunization compared with rAd-NP, which resulted in 70% protection, indicating an overall enhanced recall response in these mice (Fig. 3B). None of the mice immunized with rAd-SNP survived when challenged 4 wk postimmunization (Fig. 3A), and only 20% of the rAd-SNP–immunized mice were protected when challenged 4 mo postimmunization (Fig. 3B), indicating that secreting influenza NP (without CD40L targeting) is a less effective strategy for vaccination. Overall, these results highlight the strength of NP-based recall responses and particularly confirm that targeting Ags via CD40L could provide enhanced effective and long-lasting protection in mice.

CD40L preferentially elicits Th1-skewed, NP-specific Abs in BALB/c and C57BL/6J mice

We next determined the differences in NP-specific Ab isotypes in immunized mice. In this article, we observed that rAd-NP induced NP-specific Abs from all isotypes in both BALB/c (Fig. 4A and 4B) and C57BL/6J mice (Fig. 5A and 5B) 4 wk after primary or secondary immunization. In contrast, rAd-SNP induced up to 1-fold

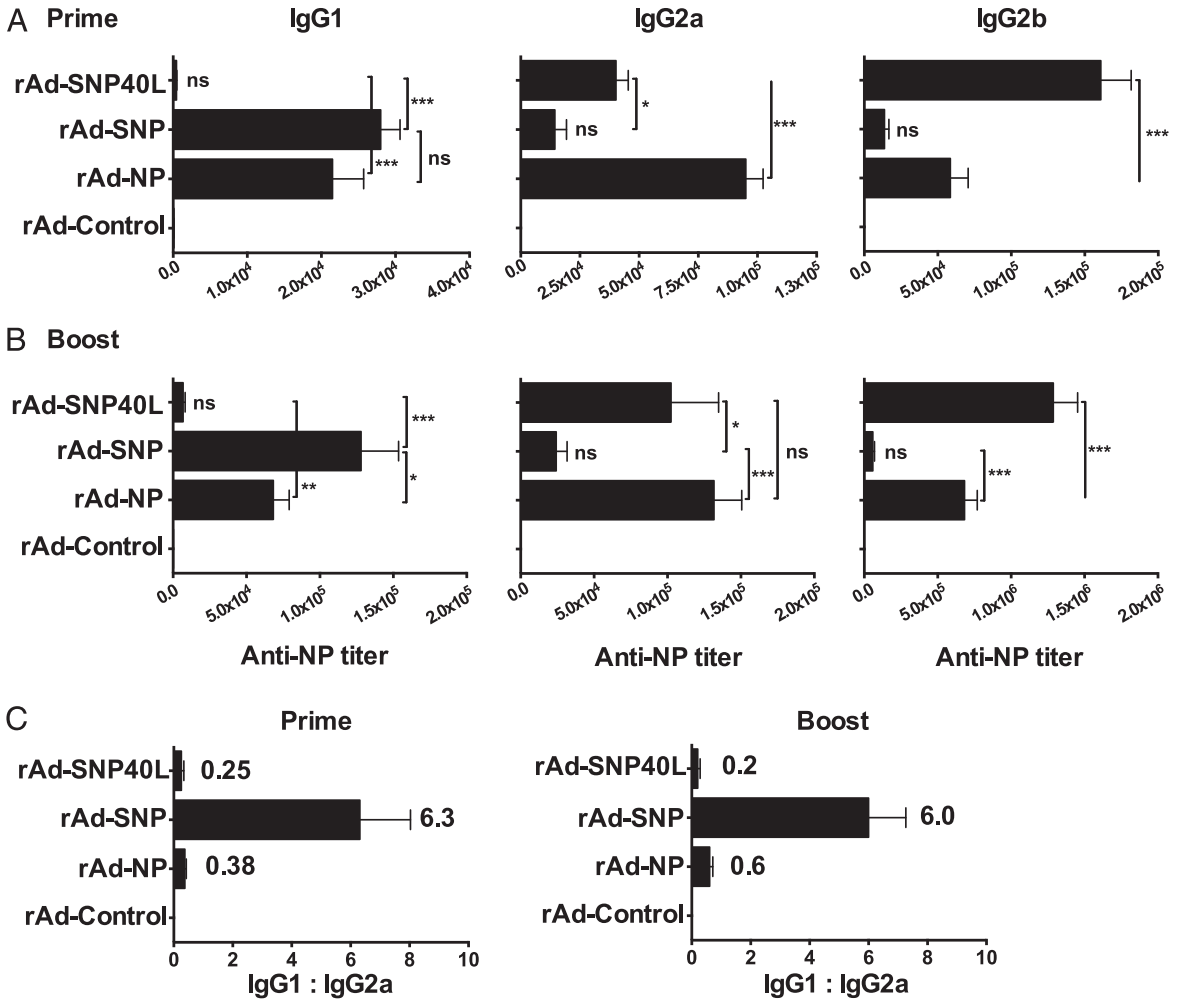

FIGURE 4. CD40 targeting preferentially induces Th1 Ab isotypes against influenza NP in wild-type BALB/c mice. Ag-specific Ab titers at 4 wk after priming (**A**) or boosting (**B**) are shown for IgG1, IgG2a, and IgG2b isotypes. (**C**) IgG1/IgG2a ratio was calculated at 4 wk after priming and boosting to determine the type of immune response (Th2 versus Th1) induced by the various constructs. Numbers on columns indicate the mean ratio. BALB/c mice were boosted at 4 wk after primary immunization. Data are shown as mean titer ± SEM from two independent experiments, with $n = 10$ mice per treatment group in each experiment. ***$p < 0.001$, **$p < 0.01$, *$p < 0.05$ (one-way ANOVA with Bonferroni posttest).

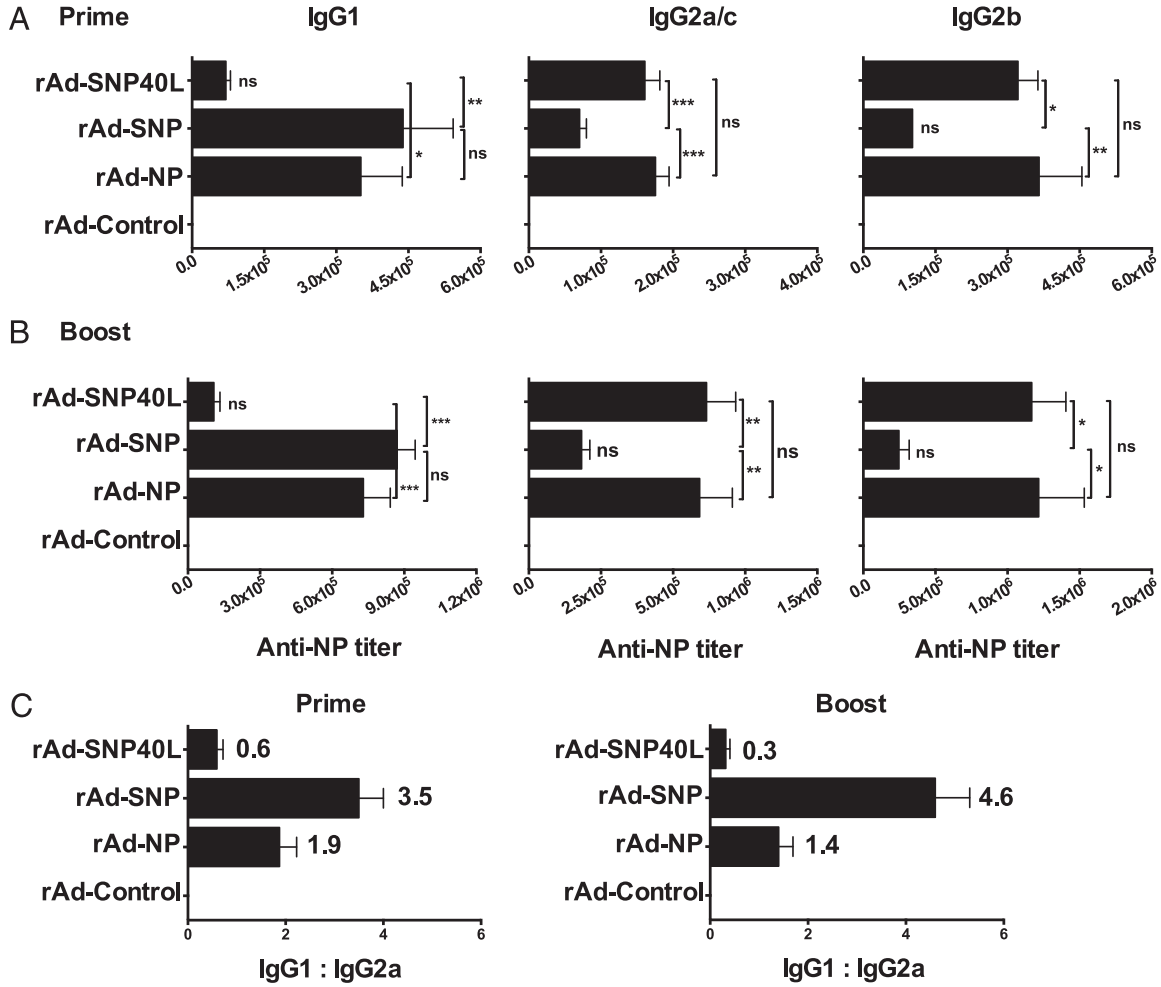

FIGURE 5. CD40 targeting preferentially induces Th1 Ab isotypes against influenza NP in wild-type C57BL/6J mice. Influenza NP-specific Ab titers at 4 wk after priming (**A**) or boosting (**B**) are shown for IgG1, IgG2a/c, and IgG2b isotypes. IgG2c was detected in C57BL/6J mice. (**C**) IgG1/IgG2a ratio was calculated at 4 wk after priming and boosting to determine the type of immune response (Th2 versus Th1) induced by the various constructs. Numbers on columns indicate the mean ratio. C57BL/6J mice were boosted at 4 wk after primary immunization. Data are shown as mean titer ± SEM from one of two experiments, with $n = 10$ mice per treatment group. $^{***}p < 0.001$, $^{**}p < 0.01$, $^{*}p < 0.05$ (one-way ANOVA with Bonferroni posttest).

higher NP-specific IgG1 Abs and markedly reduced the titers of IgG2a and IgG2b isotypes by 3- to 6- and 4- to 10-fold, respectively, in both mouse models. Targeting the secreted NP to CD40 via CD40L (rAd-SNP40L) altered the isotype ratios of NP-specific Abs by preferentially inducing IgG2a and IgG2b. Compared with rAd-NP, rAd-SNP40L reduced IgG1 levels by 10- to 20-fold and 5- to 8-fold in BALB/c (Fig. 4A and 4B) and C57BL/6J mice (Fig. 5A and 5B), respectively. As expected, empty vector (rAd-Control) failed to elicit any anti-NP Ab response. Regardless of the genetic background of BALB/c and C57BL/6J mice, which could affect the phenotype of the induced immune response (46), targeting NP via CD40L consistently elicited higher levels of IgG2b and IgG2a, and very low levels of IgG1, indicating Th1-bias, as demonstrated by the reduced IgG1/IgG2a ratios compared with rAd-NP and rAd-SNP in both mouse models (Figs. 4C and 5C).

CD40L induces early and persistent B cell GC formation and Ig isotype switching in draining LNs in BALB/c mice

Given the Th1-skewed, NP-specific Abs in sera, we next determined whether rAd-SNP40L regulates GC formation and isotype switching in draining LNs differently compared with other constructs in BALB/c mice. We first noted that rAd-SNP40L substantially altered the magnitude and the kinetics of NP-specific IgM Abs in serum. As shown in Fig. 6A, NP-specific IgM Abs in rAd-SNP40L–immunized mice peaked at day 28, albeit to low titers, and declined to low or undetectable levels by day 42, in contrast with other groups that showed significantly higher titers up to 4 wk after secondary immunization. These data suggested that rAd-SNP40L accelerated Ig isotype switching and memory B cell induction.

To further investigate the B cell development, we conducted flow cytometric analysis of B cells in draining LNs, which revealed no differences in $GL7^+$ B GC cells between the different groups until day 14 (Fig. 6B and 6C). By day 28, rAd-SNP40L–immunized mice had significantly higher frequencies of $GL7^+CD19^+$ GC B cells (25.9% of B cells) than other groups, which showed low levels of total $GL7^+CD19^+$ GC cells (3.46–5.55% of B cells). It was not until day 56 that mice in remaining groups started to show an increase in GC formation, although at lower levels compared with rAd-SNP40L–immunized mice (Fig. 6B and 6C). Further analysis also revealed significantly higher numbers of isotype-switched ($IgG^+IgD^-GL7^+$) memory B cells at days 28 (5.6% of B cells) and 42 (7.8% of B cells) in the rAd-SNP40L–immunized mice in contrast with other groups in which <1% of $CD19^+$ cells showed isotype switching (Fig. 6D). By day 56, the number of isotype-switched memory B cells in rAd-SNP40L–immunized mice was still higher than that in other groups (Fig. 6D).

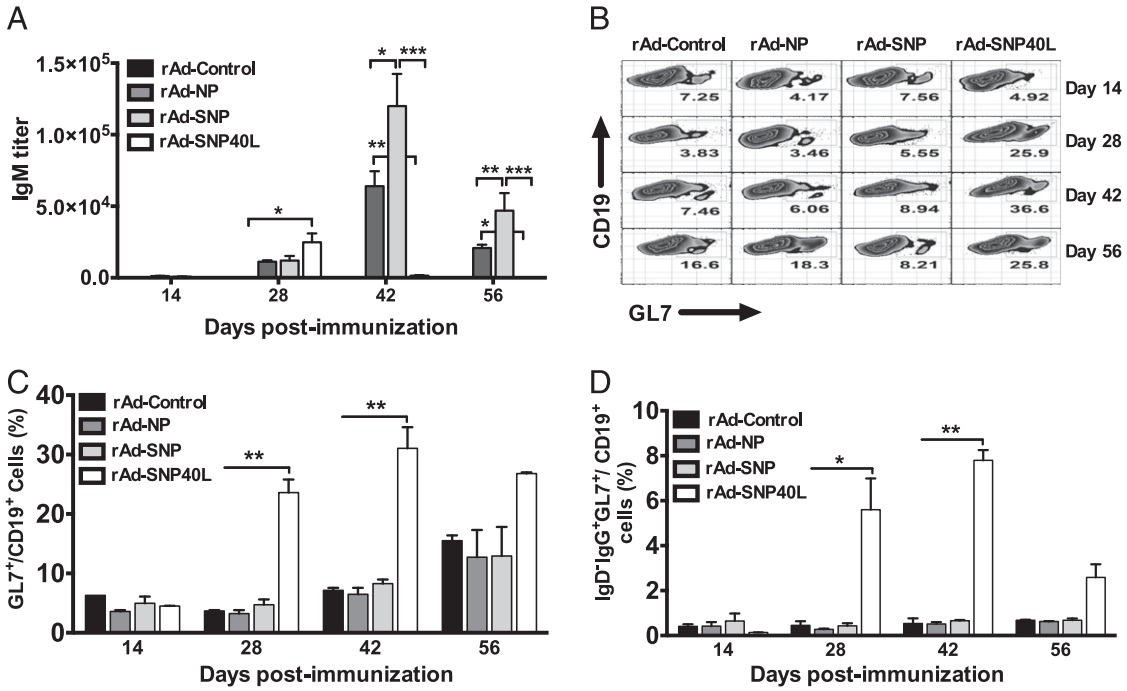

FIGURE 6. CD40L induces persistent GC and isotype-switched B cells in draining LNs of wild-type BALB/c mice. (**A**) NP-specific IgM titers were determined every 2 wk after priming and boosting in BALB/c mice. Data are shown as mean titer ± SEM from two independent experiments, with $n = 10$ mice per treatment group in each experiment. (**B**–**D**) Draining inguinal LNs were excised at indicated time points, and $CD19^+$ cells were analyzed for expression of GL7. (B) Flow cytometry plots are representatives from one of two independent experiments. (C) Graphs represent frequencies of $CD19^+$ $GL7^+$ B cells. (D) $CD19^+IgD^-IgG^+$ isotype-switched B cells were analyzed for expression of GL7 to identify isotype-switched GC cells (for gating, see Supplemental Fig. 1A). Percentage of $GL7^+$ cells and isotype-switched memory cells ($IgD^-IgG^+GL7^+$) among $CD19^+$ B cells were determined from four pooled draining LNs from each individual mouse per time point. Data are shown as mean ± SEM from two independent experiments, with $n = 2$–3 mice per treatment group per time point in each experiment. $^{***}p < 0.001$, $^{**}p < 0.01$, $^{*}p < 0.05$ (one-way ANOVA with Bonferroni posttest).

Furthermore, there was an overall upregulation of IgG and the activation markers CD40 and CD80, and a downregulation of IgD on B cells in LNs from mice immunized with CD40-targeted NP relative to other groups, particularly postsecondary immunization (Supplemental Fig. 1B and 1C). Notably, targeting influenza NP via CD40L upregulated the plasma cell marker CD138 on B cells in both the LN and spleen (Supplemental Fig. 1D and 1E) to higher levels compared with other constructs. These $CD138^+$ cells were $B220^+$ and $CD19^+$, typical of plasmablasts, confirming activation and differentiation of B cells into Ab-secreting cells in local lymphoid organs. Collectively, these data strongly suggest that there was an early and persistent induction of GC formation, as well as IgG^+ memory B cell generation in mice immunized with rAd-SNP40L.

Enhancement of NP-specific cellular immune response by CD40L in BALB/c mice

Polarization of immune response toward Th1 phenotype using CD40L (Figs. 4 and 5) suggests an induction of CTL response. Thus, we investigated the effects of CD40 targeting on NP-specific primary and secondary $CD8^+$ T cell immune responses compared with other immunogens in BALB/c mice. Upon stimulation with H-2Kd–restricted immunodominant peptide of influenza NP, we found a significant enhancement of NP-specific IL-2 (5.13%), IFN-γ (4.9%), and TNF-α (3.74%) producing $CD8^+$ T cell frequencies in spleens from mice immunized with rAd-SNP40L at 4 wk postsecondary immunization (Fig. 7A–C). In contrast, other groups showed 3- to 5-fold less cytokines producing $CD8^+$ T cells. Enhanced cytokines production was also observed 4 wk after primary immunization (Supplemental Fig. 2A–C). Because $CD8^+$ T cells capable of producing multiple cytokines (polyfunctional $CD8^+$ T cells) are a better indicator of cell-mediated immune response than single cytokine-secreting $CD8^+$ T cells (47–49), we determined the levels of these polyfunctional $CD8^+$ T cells among the different groups. We found significantly higher levels of NP-specific triple, double, and single cytokine producing $CD8^+$ T cells in rAd-SNP40L–immunized mice compared with other groups at 4 wk after primary and secondary immunization (Fig. 7D and Supplemental Fig. 2D).

To measure effector functions of NP-specific CTLs, we tested splenocytes isolated from vaccinated BALB/c mice for their ability to directly kill target cells. As shown in Fig. 7E and Supplemental Fig. 2E, rAd-SNP40L significantly increased NP-specific, cell-mediated cytotoxicity of target cells (P815 cells pulsed with MHC class I–restricted peptide). This increase in Ag-specific, cell-mediated cytotoxicity was observed as early as 2 wk after primary vaccination (data not shown). These results indicated that CD40L had not only increased specific $CD8^+$ T cell responses qualitatively, but also improved the quantity and activity of $CD8^+$ T cells as demonstrated by the significant increase in NP-specific polyfunctional $CD8^+$ T cells and CTL responses.

Both NP-specific $CD8^+$ T cells and Abs contribute to the enhanced protection in BALB/c mice

Given the findings presented earlier, we reasoned that both the NP-specific $CD8^+$ T cells and the Th1-skewed anti-NP Abs induced by CD40 targeting have contributed to the improved protection. Indeed, adoptive transfer of $CD8^+$ T cells from either rAd-NP– or rAd-SNP40L–immunized BALB/c mice significantly reduced viral replication in lungs of challenged mice by one and two logs, respectively. Notably, mice that received $CD8^+$ T cells from rAd-SNP40L–immunized group had greater reduction of virus loads in the lung compared with those that received $CD8^+$ T cells from rAd-NP–immunized mice (Fig. 8A). Moreover, after we had

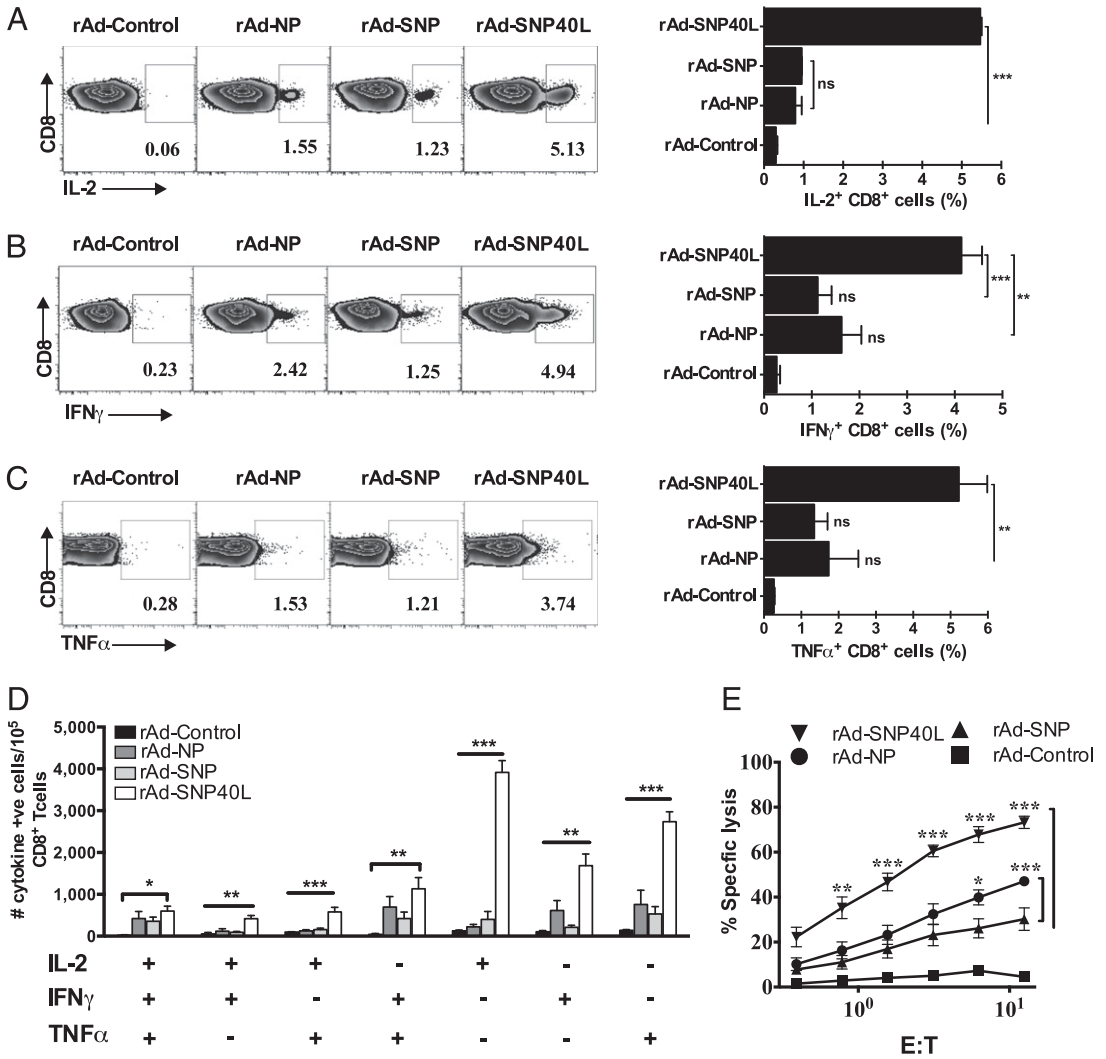

FIGURE 7. Immunization with rAd-SNP40L enhances Ag-specific memory $CD8^+$ T cell responses and cell-mediated cytotoxicity in wild-type BALB/c mice. Splenocytes isolated from immunized BALB/c mice 4 wk after secondary vaccination were restimulated ex vivo with synthetic NP peptide. $CD8^+$ T cells were then stained for intracellular IL-2, IFN-γ, and TNF-α cytokines. Graphs represent frequencies of (**A**) IL-2–, (**B**) IFN-γ–, and (**C**) TNF-α–producing $CD8^+$ T cells. Flow cytometry plots are representatives from one out of two independent experiments. (**D**) Analysis of single-, double-, and triple-cytokine–producing $CD8^+$ T cells 4 wk after boosting. Bar graphs represent frequencies of various combinations of cytokine-producing cells normalized to represent cytokine-producing cell numbers per 100,000 cells. (**E**) Splenocytes were cultured ex vivo with synthetic NP peptide to generate effector cells. NP-specific cytotoxic activity was measured at different E:T ratios, and the percentage of specific lysis was calculated. Data are shown as mean ± SEM from two independent experiments, with $n = 2$–3 mice per treatment group in each experiment. $^{***}p < 0.001$, $^{**}p < 0.01$, $^{*}p < 0.05$ [one-way ANOVA in (A)–(D), and two-way ANOVA in (E) with Bonferroni posttest for both].

passively transferred sera from vaccinated wild-type BALB/c mice into naive mice, we observed that mice that received pooled sera from rAd-SNP40L–immunized mice showed significantly lower viral titers (more than one log) in their lungs after lethal viral challenge compared with other groups (Fig. 8B). These results are consistent with a model in which rAd-SNP40L immunization enhanced protection by augmenting the roles of both $CD8^+$ T cells and NP-specific Abs.

Enhanced protection is mediated through CD40 targeting

To confirm that the enhanced rAd-SNP40L protection observed in the animal studies is indeed mediated through CD40-CD40L

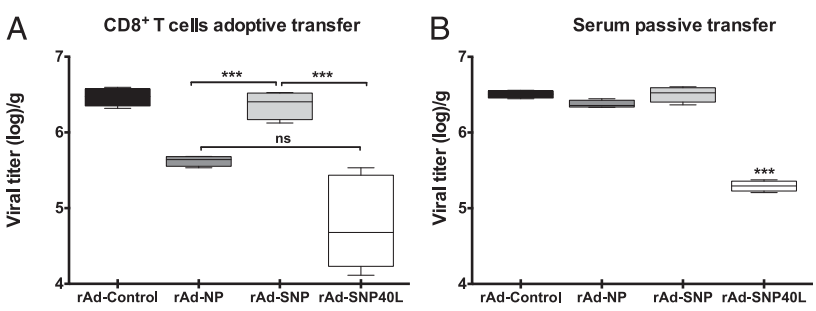

FIGURE 8. Targeting influenza NP to $CD40^+$ cells improves the protection afforded by both $CD8^+$ T cells and NP-specific Abs in wild-type BALB/c mice. Naive BALB/c mice ($n = 4$ per group) received (**A**) 1×10^7 purified $CD8^+$ T cells or (**B**) serum from vaccinated donor mice was challenged with $10\times$ LD_{50} of influenza A/Puerto Rico/8/34(H1N1) virus. Lung viral titer was measured on day 6 postchallenge. Data are shown as mean titer ± SEM. $^{***}p < 0.001$ (one-way ANOVA with Bonferroni posttest).

ligation, we investigated the protective efficacy of rAd-SNP40L in a CD40L$^{-/-}$ mouse model. As expected, all vaccinated mice, regardless of the type of rAd, generated weak NP-specific IgM Abs and barely detectable IgG Abs (Supplemental Fig. 3), supporting the role of CD40L in promoting Ig isotype switching. However, when these mice were challenged with influenza virus, all mice immunized with rAd-SNP40L were protected from lethal viral challenge, which was accompanied by significantly less weight loss and better clinical scores (Fig. 9A). Noticeably, even though CD40L does not seem to reconstitute the immune system in this mouse model for Ig isotype switching (see *Discussion*), these data demonstrate that the improved protective immune response against influenza is largely mediated through CD40–CD40L interaction.

CD40L induces CD4$^+$ T cell–independent immune response and protection against influenza

Next, we examined the role of, and the need for, CD4$^+$ T cells during immune response induction in rAd-SNP40L immunization. To this end, CD4$^{-/-}$ mice were used in these animal experiments. When immunized mice were challenged with 5× LD_{50} of influenza virus, only 20–25% of rAd-NP or rAd-SNP vaccinated mice survived, whereas all mice immunized with rAd-SNP40L survived the challenge and maintained their body weight with less severe clinical symptoms (Fig. 9B). Mechanistically, CD4$^{-/-}$ mice failed to mount a significant Ab response to rAd-NP or rAd-SNP vaccination (Fig. 10A and 10B). Specifically, IgG2a/c and IgG2b isotypes in rAd-NP immunized CD4$^{-/-}$ mice were lower by 65- to 70- and 40- to 52-fold, respectively, after primary or secondary immunization compared with C57BL/J6 wild-type mice (Table I). Reduction in Ab response in CD4$^{-/-}$ was most prominent in the IgG1 isotype upon immunization with either rAd-NP or rAd-SNP, as shown in Table I, suggesting a critical role for CD4$^+$ T cells in IgG1 production. As expected, the difference in IgG2a/c and IgG2b Abs was less pronounced in rAd-SNP immunized mice because rAd-SNP vaccination induces mainly IgG1 and very low levels of these two isotypes in wild-type C57BL/J6 mice (Fig. 5). In sharp contrast, immunization with rAd-SNP40L induced high levels of anti-NP Abs, comparable with those observed in wild-type mice (Fig. 10A and 10B), with only a 3- to 15-fold difference between all the isotypes (Table I). Interestingly, the Ab isotypes in CD4$^{-/-}$ mice were skewed toward Th1 response (IgG2a/c and IgG2b) in a similar manner to that of wild-type C57BL/J6 mice. Taken together, these data indicate that CD40 targeting via CD40L induced CD4$^+$ T cell–independent Th1-skewed immune response and afforded full protection against lethal influenza challenge in CD4$^{-/-}$-immunodeficient animals.

CD8$^+$ T cells are indispensable in NP-based protection against influenza

Finally, we tried to investigate the importance of CD8$^+$ T cells in the observed rAd-SNP40L–mediated protection. Interestingly, none of the constructs conferred any protection in the immunized mice, as shown in Fig. 11. All vaccinated mice suffered severe clinical symptoms similar to the control group and died within 7–9 d postchallenge. These results are consistent with previous reports and the important role of CD8$^+$ T cells in NP-based protection against influenza. They also suggest that even though both NP-specific Abs and CD8$^+$ T cells are involved in rAd-SNP40L–mediated protection, CD8$^+$ T cells are the main players in the observed protection (Fig. 11).

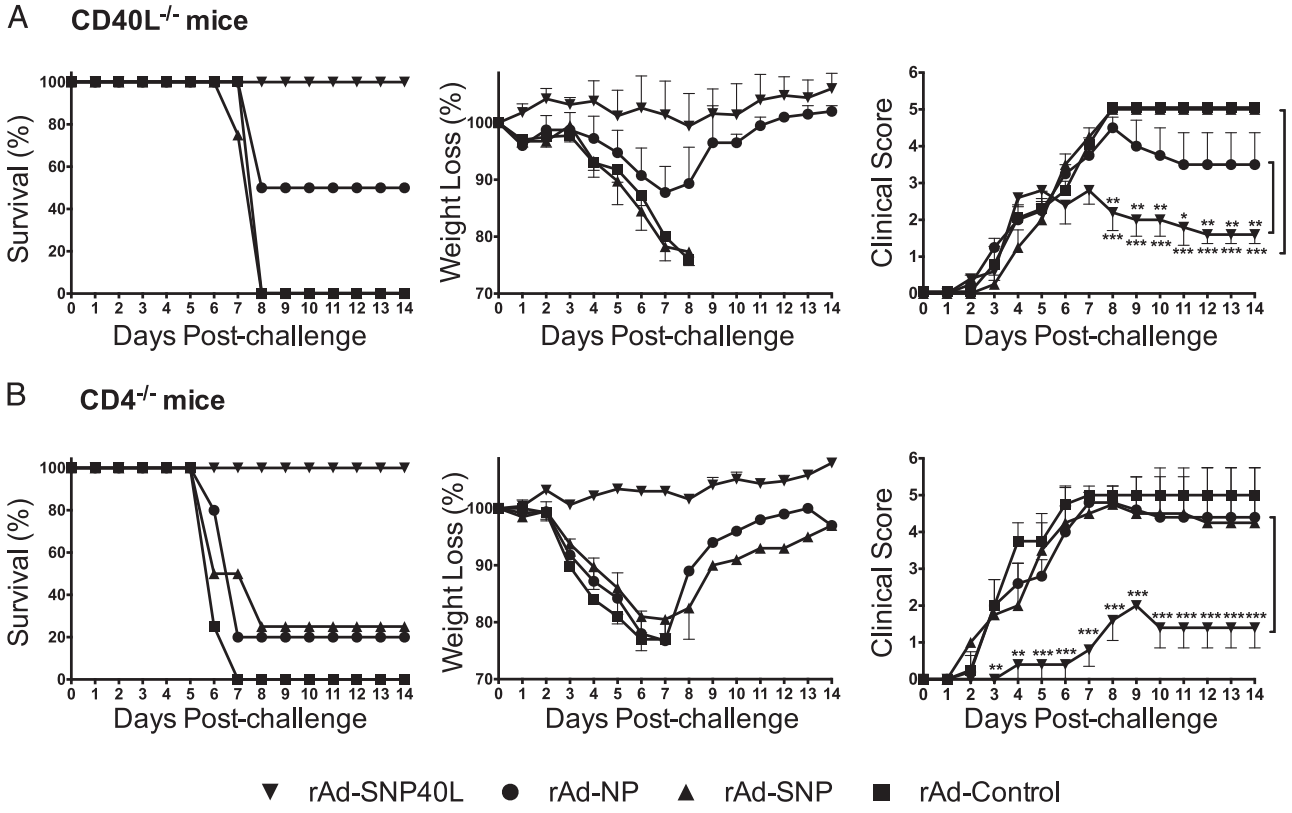

FIGURE 9. Immunization with rAd-SNP40L enhances protection in CD40L$^{-/-}$ and CD4$^{-/-}$ mice. Survival curves, body weight loss, and clinical score were presented in (**A**) CD40L$^{-/-}$ and (**B**) CD4$^{-/-}$ mice. Animals were challenged with 5× LD_{50} of influenza A/Puerto Rico/8/34(H1N1) virus 4 wk after secondary immunization. Both knockout mouse models are on C57BL/6J genetic background. Data are shown from one experiment with $n = 4$–5 mice per treatment group. ***$p < 0.001$, **$p < 0.01$, *$p < 0.05$ (two-way ANOVA with Bonferroni posttest).

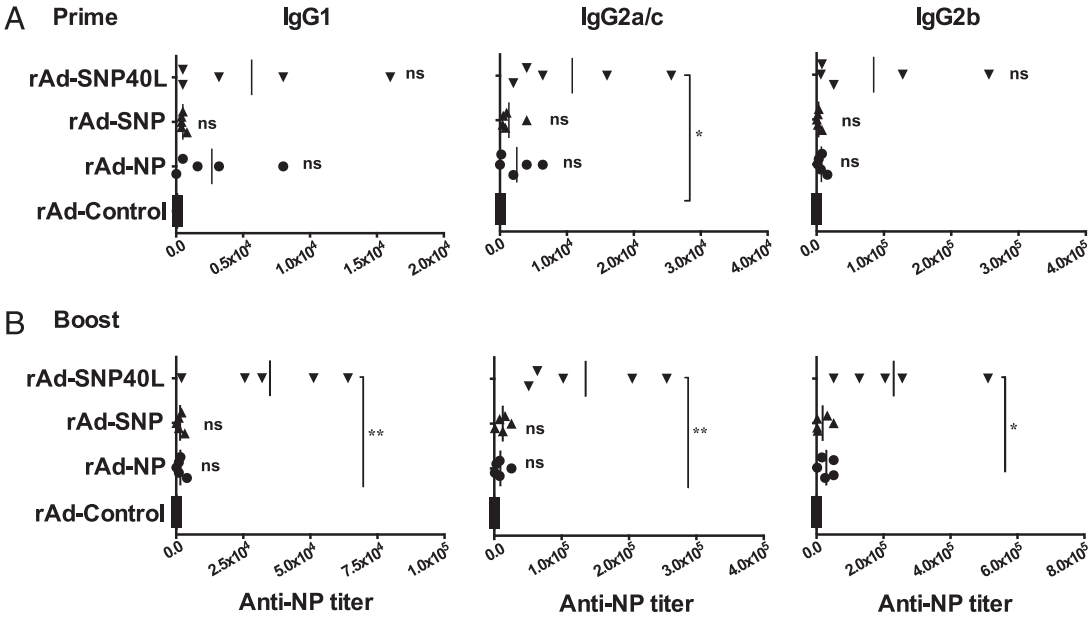

FIGURE 10. Immunization with rAd-SNP40L induces CD4-indepdendent Ab responses against influenza NP in CD4$^{-/-}$ mice. Influenza NP-specific Ab titers at 4 wk after (**A**) priming and (**B**) boosting are shown for IgG1, IgG2a/c, and IgG2b isotypes. IgG2c was detected in CD4$^{-/-}$ mice. CD4$^{-/-}$ mice were boosted at 4 wk postprimary immunization. CD4$^{-/-}$ mice are on C57BL/6J genetic background. Data are shown as mean titer ± SEM from one experiment, with $n = 5$ mice per treatment group. $^{**}p < 0.01$, $^{*}p < 0.05$ (one-way ANOVA with Bonferroni posttest).

Discussion

Although several studies have used CD40L as a molecular adjuvant codelivered with Ags of interest using plasmid DNA or viral vectors, or as an adaptor protein to alter the tropism of delivery vectors, several reasons have prompted us to investigate the effect of CD40L on influenza NP-induced immunity. First, although CD40L was reported to enhance the humoral immune response against HA, it provided only partial protection with multiple doses (26, 30). Second, the internal protein NP, albeit a much more conserved protein (>94% homology), is a much weaker protective Ag compared with HA because NP immunization cannot prevent infection or the occurrence of mild symptoms. Thus, NP would represent a good candidate Ag to investigate the potential of CD40L on NP-specific immune response. Third, we wished to dissect the functional roles of the nonneutralizing Abs and T cell subsets in protection.

The transgene was designed to encode a secreted fusion protein targeted to CD40 receptors on APCs to achieve these goals. Initial experiments showed that the construct missing the S, designated as rAd-NP40L, is unable to induce any immune response or afford any protection against influenza challenge, underscoring the importance of the secretion of the fusion protein. It could be envisaged that because many cell types are susceptible to adenovirus infection including proliferating and nonproliferating cells (23, 27), gene products with S produced by the adenovirus-infected cells would increase the Ag loads in vivo (Fig. 12). Furthermore, because the fusion protein is targeted to CD40 on APCs, immune response against NP is expected to be amplified because of CD40-CD40L ligation. Although APCs themselves are relatively refractory to adenovirus infection because of their lack of its main receptor, coxsackie-adenovirus receptor (CAR), direct infection of these cells through different receptors or alternative mechanisms (50) can not only promote their own maturation, but can also result in secretion of the fusion protein into regional LNs and direct activation of T and B cells. Thus, CD40L can act as an adjuvant and targeting molecule in both the peripheries (sites of injection) and/or the secondary lymphoid organs, as illustrated in Fig. 12.

The finding that the three constructs (rAd-NP, rAd-SNP, and rAd-SNP40L) elicited differently skewed immune responses is noteworthy. Secreted NP after rAd-SNP injection resulted in Th2-skewed responses, as suggested by increased levels of NP-specific IgG1 Abs and reduced levels of the other isotypes. However, targeting the secreted NP to CD40^{+} cells via CD40L significantly induced Th1-biased, NP-specific Ab response. This dramatic shift from Th2 to Th1 was observed in both MHC haplotypes H-2d (BALB/c) and H-2b (C57BL/6J), and manifested by increased IgG2a/c and IgG2b, and reduced IgG1 isotype levels. Moreover, rAd-SNP40L preferentially altered the kinetics of B cell responses by promoting early and long-lasting GC formation, plasma cells induction, and isotype-switched memory B cell generation in draining LNs by day 28. In addition, targeting secreted NP via CD40L enhanced T cell responses as demonstrated

Table I. Fold difference in Ab response between wild-type C57BL/6J and B6.129S2-Cd4^{tm1Mak}/J (CD4$^{-/-}$) mice

	Primary Immunization			Secondary Immunization		
Ab Isotype	rAd-NP	rAd-SNP	rAd-SNP40L	rAd-NP	rAd-SNP	rAd-SNP40L
IgG1	132	878	12	474	596	3
IgG2a/c	70	53	15	65	14	5
IgG2b	52	33	4	40	14	5

See also Figs. 3 and 10.

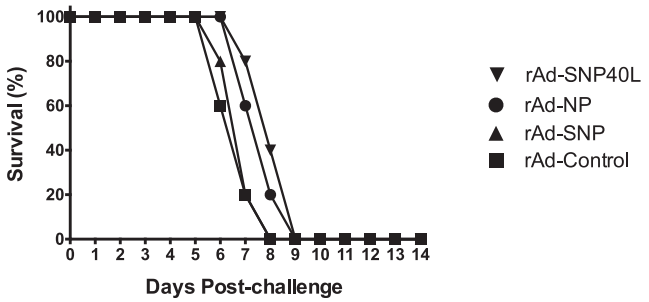

FIGURE 11. $CD8^+$ T cells are crucial in NP-based protection against influenza. Survival curves of $CD8^{-/-}$ mice immunized with two doses of 10^9 PFU of the indicated rAd constructs and challenged with 5× LD_{50} of mouse-adapted influenza A/Puerto Rico/8/1934(H1N1) virus 4 wk after secondary immunization are shown. Data are shown from one experiment with $n = 5$ mice per treatment group.

by robust NP-specific CTL response as early as 14 d after primary immunization. It also improved the quality of $CD8^+$ T cells by significantly increasing the frequencies of polyfunctional $CD8^+$ T cells, which are known to be superior in mediating protection against infections and as a surrogate marker for the quality of vaccine-induced T cells responses (47–49). Taken together, the immune response was markedly enhanced in rAd-SNP40L–immunized mice at all levels, which explains the conferred heterosubtypic protection in BALB/c and C57BL/6J mice, and the long-lasting protection even after a single dose of rAd-SNP40L. To our knowledge, there has been no report of NP-based vaccination capable of inducing such a strong protection against influenza.

The observation that both $CD8^+$ T cells and Abs can reduce viral replication in the recipient mice in the adoptive and passive transfer studies provided additional mechanistic insight into the rAd-SNP40L vaccination. Although experiments involving depletion of $CD8^+$ T cells or B cells in vaccinated mice may shed light on the importance and the role of these two arms of the immune system in protection, the fact that none of the rAds used in this study was able to confer any protection in $CD8^{-/-}$ mice (Fig. 11) suggests that $CD8^+$ T cells are indispensable in NP-based protection against influenza. Notably, passive transfer of anti-NP sera from rAd-NP– or rAd-SNP–immunized groups failed to convey protection to recipient mice, consistent with the suggestion that normal mice, not like B cell–deficient ($\mu MT^{-/-}$) mice, require high levels of anti-NP Abs for protection (51). In contrast, sera from rAd-SNP40L immunized mice significantly reduced lung viral load, suggesting a correlation between the shift in Ab isotypes and the inhibition of viral replication. Indeed, Th1-related Abs, IgG2a/c and IgG2b, are associated with effector mechanisms such as FcRs binding, complement-fixation, or complement-mediated lysis of infected cells (52, 53), even though NP-Abs are not neutralizing Abs.

Vaccination of $CD40L^{-/-}$ mice with rAd-SNP40L elicited NP-specific IgM response, accompanied with very low levels of IgG2b isotype, which is very similar to rAd-NP– and rAd-SNP–immunized groups (Supplemental Fig. 3). These results suggest that the levels of CD40L produced by the transient expression from rAd-SNP40L–infected cells is insufficient to restore isotype-switching in these mice. This is consistent with previous studies showing that constitutive expression of CD40L (54) or coadministration of high doses of rCD40L (50 mg given 3 times/week), but not lower doses (5 mg given 3 times/week) (55), can only induce low to intermediate levels of Ag-specific isotype-switched Abs in $CD40L^{-/-}$ mice. Nevertheless, rAd-SNP40L immunization completely protected $CD40L^{-/-}$ mice against influenza challenge, most likely through CTL response, as our data suggest that $CD8^+$ T cells play critical roles in protection (Figs. 8 and 11).

The role of $CD4^+$ T cells was critical because rAd-NP– and rAd-SNP–immunized $CD4^{-/-}$ mice failed to mount a strong Ab response against influenza. In contrast, rAd-SNP40L–immunized $CD4^{-/-}$ mice showed increased production of all isotypes, including IgG1 Abs, to levels very similar to those observed in wild-type mice with a 4- to 7-fold difference only (Table I). Interestingly, like in the wild-type C57BL/6J mice, rAd-SNP40L induced a Th1-polarized response in $CD4^{-/-}$ mice. This observation is different from a study that showed Th2-skewed response in CD4-depleted mice and balanced Th1/Th2 response in $CD4^{-/-}$ mice

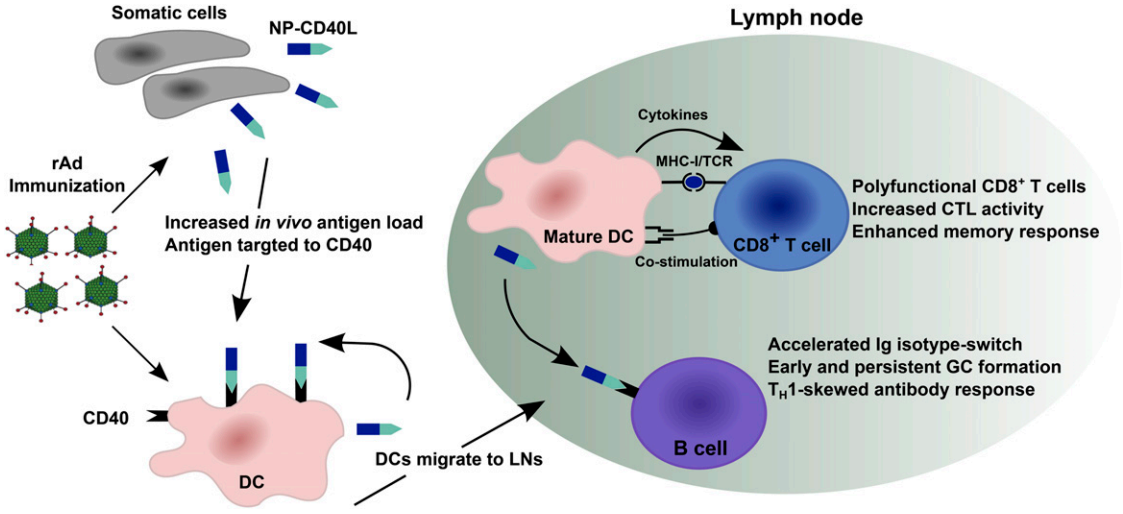

FIGURE 12. Schematic model of immune response induction using CD40-targeted Ag. Subcutaneous immunization with rAd-encoding SNP-CD40L fusion protein results in infection of proliferating and nonproliferating cells; thus, secreted gene products increase the Ag loads in vivo at the site of injection. The fusion protein then binds to CD40 on APCs via CD40L to initiate immune response induction and amplification. DCs can also be directly infected with rAd, leading to their maturation into professional APCs and subsequent secretion of the fusion protein into regional LNs to directly activate B cells. Thus, CD40L can act as an adjuvant and targeting molecule in both the peripheries and/or the secondary lymphoid organs. In the LNs, the CD40L-activated DCs activate Ag-specific $CD8^+$ T cells to induce enhanced CTL activity and multiple cytokines producing cytotoxic T cells. Meanwhile, secreted CD40-targeted Ags activate B cells and elicit accelerated Ig isotype switch, early and persistent GC formation, and Th1-skewed Ab response.

(17). Although we cannot fully explain the difference between the two studies at this time, such a discrepancy could be because of the difference in immunization regimens used in both studies. Specifically, whereas we used two doses of rAd to target the encoded Ag as a fusion protein directly to $CD40^+$ APCs via CD40L, Zheng and colleagues (17) codelivered CD40L with Ag through a coimmunization or coexpression using DNA prime/rAd boost approach. Nonetheless, data reported by Zheng et al. (17) clearly show that using CD40L as an adjuvant can effectively induce significant levels of protective Abs and $CD8^+$ T cells in a $CD4^+$ T cell–independent manner. Furthermore, Auten et al. (20) showed that coexpression or coimmunization of CD40L together with mycobacterial protein Ag 85B in a plasmid DNA prime/rAd boost regimen can restore vaccine-induced circulating and mucosal $CD4^+$ and $CD8^+$ T cell responses in $CD4^+$ T cell–depleted mice. Although we only examined Ab titers, but not $CD8^+$ T cell response, in immunized $CD4^{-/-}$ mice, the observation that none of the constructs generated in this study was able to confer any protection in $CD8^{-/-}$ mice (Fig. 11) indicate that both humoral and cellular responses are involved and can be induced by using CD40L in $CD4^{-/-}$ mice (Fig. 12).

The significance of these results is paramount in regard to immunodeficiency. There is a growing need to develop new strategies to elicit CD4-indpendent immune responses or at least to partially substitute for $CD4^+$ T cell loss in immunocompromised individuals with defective $CD4^+$ T cells or CD40L deficiency. For example, in HIV infection, the gradual loss of virus-specific $CD4^+$ T cells is associated with significant reduction in CD40L expression (56, 57). Similarly, it was shown that age-related reduction in CD40L levels is associated with the defects in cognate $CD4^+$ T cell function, thus weakening humeral response in aged individuals (58). Such defects do not only result in impaired immune responses and increased risk for opportunistic infections but also in drastically reduced efficacy of vaccination (59). Although it would be of great interest to test this vaccine in an aged mouse model in future studies, our data demonstrate that targeting Ags via CD40L may overcome such defects and induce protective immune response in hosts with either $CD4^+$ T cell or CD40L immunodeficiency.

Current influenza vaccines mostly induce immune responses against the highly variable regions of the HA and NA (60, 61). Therefore, these strategies may not lead to heterosubtypic protection against the divergent influenza subtypes. However, the highly conserved internal proteins such as NP have been shown to induce effective immune responses and provide protection against various influenza A subtypes in several animal models (32–34, 62–64). Yet, NP-based vaccination has been shown to be associated with limited protection in other studies (35–37). Noticeably, Roy et al. (65) showed that a single i.m. immunization with human adenovirus serotype 5 or the chimpanzee adenovirus serotype 7 expressing influenza A/Puerto Rico/8/34(H1N1) NP can elicit a strong T cell response and 90–100% protection against a homologs challenge. However, significant heterosubtypic protection (40–80%) was observed only against influenza A/Vietnam/1203/04 (H5N1) virus, but not influenza A/Hong Kong/483/97(H5N1). In our study, we found that using CD40L as adjuvant and targeting molecule can enhance the breadth, potency, and durability of NP-specific immune responses, as well as the protection not in normal mice only but also in $CD4^{-/-}$ and $CD40L^{-/-}$ mice. Although we focused on vaccination using influenza NP, this work points toward a broadly applicable, effective means of inducing durable immune response and protection. Further studies are currently ongoing to determine the potential of this platform to improve the immunogenicity and protective efficacy of other Ags. To our knowledge, this is the first report demonstrating that a single dose of NP-based immunization can elicit strong and long-lasting protective immune responses against influenza involving both $CD8^+$ T cells and anti-NP Abs.

Acknowledgments

We thank Louise Larocque, Marsha Russell, Emily Chomyshyn, and Michelle Lemieux for technical assistance. We are so grateful to Dr. Martha Navarro and all technicians in the animal facility for help. Drs. Aaron Farnsworth and Daryl Smith (Health Canada) are acknowledged for their critical review of the manuscript.

Disclosures

The authors have no financial conflicts of interest.

References

1. Kovacsovics-Bankowski, M., K. Clark, B. Benacerraf, and K. L. Rock. 1993. Efficient major histocompatibility complex class I presentation of exogenous antigen upon phagocytosis by macrophages. *Proc. Natl. Acad. Sci. USA* 90: 4942–4946.
2. Guermonprez, P., J. Valladeau, L. Zitvogel, C. Théry, and S. Amigorena. 2002. Antigen presentation and T cell stimulation by dendritic cells. *Annu. Rev. Immunol.* 20: 621–667.
3. Whitmire, J. K., and R. Ahmed. 2000. Costimulation in antiviral immunity: differential requirements for CD4(+) and CD8(+) T cell responses. *Curr. Opin. Immunol.* 12: 448–455.
4. van Kooten, C., and J. Banchereau. 2000. CD40-CD40 ligand. *J. Leukoc. Biol.* 67: 2–17.
5. Bishop, G. A., and B. S. Hostager. 2003. The CD40-CD154 interaction in B cell-T cell liaisons. *Cytokine Growth Factor Rev.* 14: 297–309.
6. Quezada, S. A., L. Z. Jarvinen, E. F. Lind, and R. J. Noelle. 2004. CD40/CD154 interactions at the interface of tolerance and immunity. *Annu. Rev. Immunol.* 22: 307–328.
7. Ma, D. Y., and E. A. Clark. 2009. The role of CD40 and CD154/CD40L in dendritic cells. *Semin. Immunol.* 21: 265–272.
8. Bennett, S. R., F. R. Carbone, F. Karamalis, R. A. Flavell, J. F. Miller, and W. R. Heath. 1998. Help for cytotoxic-T-cell responses is mediated by CD40 signalling. *Nature* 393: 478–480.
9. Schoenberger, S. P., R. E. Toes, E. I. van der Voort, R. Offringa, and C. J. Melief. 1998. T-cell help for cytotoxic T lymphocytes is mediated by CD40-CD40L interactions. *Nature* 393: 480–483.
10. Ahmed, K. A., L. Wang, M. A. Munegowda, S. J. Mulligan, J. R. Gordon, P. Griebel, and J. Xiang. 2012. Direct in vivo evidence of CD4+ T cell requirement for CTL response and memory via pMHC-I targeting and CD40L signaling. [Published erratum appears in 2012 *J. Leukoc. Biol.* 92: 1123.] *J. Leukoc. Biol.* 92: 289–300.
11. Schultze, J. L., S. Michalak, M. J. Seamon, G. Dranoff, K. Jung, J. Daley, J. C. Delgado, J. G. Gribben, and L. M. Nadler. 1997. CD40-activated human B cells: an alternative source of highly efficient antigen presenting cells to generate autologous antigen-specific T cells for adoptive immunotherapy. *J. Clin. Invest.* 100: 2757–2765.
12. Lapointe, R., A. Bellemare-Pelletier, F. Housseau, J. Thibodeau, and P. Hwu. 2003. CD40-stimulated B lymphocytes pulsed with tumor antigens are effective antigen-presenting cells that can generate specific T cells. *Cancer Res.* 63: 2836–2843.
13. Mendoza, R. B., M. J. Cantwell, and T. J. Kipps. 1997. Immunostimulatory effects of a plasmid expressing CD40 ligand (CD154) on gene immunization. *J. Immunol.* 159: 5777–5781.
14. Gurunathan, S., K. R. Irvine, C. Y. Wu, J. I. Cohen, E. Thomas, C. Prussin, N. P. Restifo, and R. A. Seder. 1998. CD40 ligand/trimer DNA enhances both humoral and cellular immune responses and induces protective immunity to infectious and tumor challenge. *J. Immunol.* 161: 4563–4571.
15. Tripp, R. A., L. Jones, L. J. Anderson, and M. P. Brown. 2000. CD40 ligand (CD154) enhances the Th1 and antibody responses to respiratory syncytial virus in the BALB/c mouse. *J. Immunol.* 164: 5913–5921.
16. Sin, J. I., J. J. Kim, D. Zhang, and D. B. Weiner. 2001. Modulation of cellular responses by plasmid CD40L: CD40L plasmid vectors enhance antigen-specific helper T cell type 1 CD4+ T cell-mediated protective immunity against herpes simplex virus type 2 in vivo. *Hum. Gene Ther.* 12: 1091–1102.
17. Zheng, M., A. J. Ramsay, M. B. Robichaux, K. A. Norris, C. Kliment, C. Crowe, R. R. Rapaka, C. Steele, F. McAllister, J. E. Shellito, et al. 2005. CD4+ T cell-independent DNA vaccination against opportunistic infections. *J. Clin. Invest.* 115: 3536–3544.
18. Gómez, C. E., J. L. Nájera, R. Sánchez, V. Jiménez, and M. Esteban. 2009. Multimeric soluble CD40 ligand (sCD40L) efficiently enhances HIV specific cellular immune responses during DNA prime and boost with attenuated poxvirus vectors MVA and NYVAC expressing HIV antigens. *Vaccine* 27: 3165–3174.
19. Cao, J., X. Wang, Y. Du, Y. Li, X. Wang, and P. Jiang. 2010. CD40 ligand expressed in adenovirus can improve the immunogenicity of the GP3 and GP5 of porcine reproductive and respiratory syndrome virus in swine. *Vaccine* 28: 7514–7522.

20. Auten, M. W., W. Huang, G. Dai, and A. J. Ramsay. 2012. CD40 ligand enhances immunogenicity of vector-based vaccines in immunocompetent and CD4+ T cell deficient individuals. *Vaccine* 30: 2768–2777.
21. Manoj, S., P. J. Griebel, L. A. Babiuk, and S. van Drunen Littel-van den Hurk. 2004. Modulation of immune responses to bovine herpesvirus-1 in cattle by immunization with a DNA vaccine encoding glycoprotein D as a fusion protein with bovine CD154. *Immunology* 112: 328–338.
22. Pereboev, A. V., J. M. Nagle, M. A. Shakhmatov, P. L. Triozzi, Q. L. Matthews, Y. Kawakami, D. T. Curiel, and J. L. Blackwell. 2004. Enhanced gene transfer to mouse dendritic cells using adenoviral vectors coated with a novel adapter molecule. *Mol. Ther.* 9: 712–720.
23. Huang, D., A. V. Pereboev, N. Korokhov, R. He, L. Larocque, C. Gravel, B. Jaentschke, M. Tocchi, W. L. Casley, M. Lemieux, et al. 2008. Significant alterations of biodistribution and immune responses in Balb/c mice administered with adenovirus targeted to CD40(+) cells. *Gene Ther.* 15: 298–308.
24. Lin, F. C., Y. Peng, L. A. Jones, P. H. Verardi, and T. D. Yilma. 2009. Incorporation of CD40 ligand into the envelope of pseudotyped single-cycle Simian immunodeficiency viruses enhances immunogenicity. *J. Virol.* 83: 1216–1227.
25. Hangalapura, B. N., D. Oosterhoff, S. Aggarwal, P. G. J. T. B. Wijnands, R. van de Ven, S. J. A. M. Santegoets, M. P. van den Tol, E. Hooijberg, A. Pereboev, A. J. M. van den Eertwegh, et al. 2010. Selective transduction of dendritic cells in human lymph nodes and superior induction of high-avidity melanoma-reactive cytotoxic T cells by a CD40-targeted adenovirus. *J. Immunother.* 33: 706–715.
26. Yao, Q., K. P. Fischer, L. Li, B. Agrawal, Y. Berhane, D. L. Tyrrell, K. S. Gutfreund, and J. Pasick. 2010. Immunogenicity and protective efficacy of a DNA vaccine encoding a chimeric protein of avian influenza hemagglutinin subtype H5 fused to CD154 (CD40L) in Pekin ducks. *Vaccine* 28: 8147–8156.
27. Kim, Y.-S., Y.-J. Kim, J.-M. Lee, S.-H. Han, H.-J. Ko, H.-J. Park, A. Pereboev, H. H. Nguyen, and C.-Y. Kang. 2010. CD40-targeted recombinant adenovirus significantly enhances the efficacy of antitumor vaccines based on dendritic cells and B cells. *Hum. Gene Ther.* 21: 1697–1706.
28. Franco, D., W. Liu, D. F. Gardiner, B. H. Hahn, and D. D. Ho. 2011. CD40L-containing virus-like particle as a candidate HIV-1 vaccine targeting dendritic cells. *J. Acquir. Immune Defic. Syndr.* 56: 393–400.
29. Hangalapura, B. N., D. Oosterhoff, J. de Groot, L. Boon, T. Tüting, A. J. van den Eertwegh, W. R. Gerritsen, V. W. van Beusechem, A. Pereboev, D. T. Curiel, et al. 2011. Potent antitumor immunity generated by a CD40-targeted adenoviral vaccine. *Cancer Res.* 71: 5827–5837.
30. Sánchez Ramos, O., A. González Pose, S. Gómez-Puerta, J. Noda Gomez, A. Vega Redondo, J. C. Águila Benites, L. Suárez Amarán, N. C. Parra, and J. R. Toledo Alonso. 2011. Avian CD154 enhances humoral and cellular immune responses induced by an adenovirus vector-based vaccine in chickens. *Comp. Immunol. Microbiol. Infect. Dis.* 34: 259–265.
31. Hashem, A., T. M. Doyle, G. Van Domselaar, A. Farnsworth, C. Li, J. Wang, R. He, and X. Li. 2011. Recent developments in bioinformatics analyses of influenza A virus surface glycoproteins and their biological relevance. *Curr. Bioinform.* 6: 415–426.
32. Fu, T. M., A. Friedman, J. B. Ulmer, M. A. Liu, and J. J. Donnelly. 1997. Protective cellular immunity: cytotoxic T-lymphocyte responses against dominant and recessive epitopes of influenza virus nucleoprotein induced by DNA immunization. *J. Virol.* 71: 2715–2721.
33. Epstein, S. L., W.-P. Kong, J. A. Misplon, C.-Y. Lo, T. M. Tumpey, L. Xu, and G. J. Nabel. 2005. Protection against multiple influenza A subtypes by vaccination with highly conserved nucleoprotein. *Vaccine* 23: 5404–5410.
34. Laddy, D. J., J. Yan, A. S. Khan, H. Andersen, A. Cohn, J. Greenhouse, M. Lewis, J. Manischewitz, L. R. King, H. Golding, et al. 2009. Electroporation of synthetic DNA antigens offers protection in nonhuman primates challenged with highly pathogenic avian influenza virus. *J. Virol.* 83: 4624–4630.
35. Patel, A., K. Tran, M. Gray, Y. Li, Z. Ao, X. Yao, D. Kobasa, and G. P. Kobinger. 2009. Evaluation of conserved and variable influenza antigens for immunization against different isolates of H5N1 viruses. *Vaccine* 27: 3083–3089.
36. Rao, S. S., W.-P. Kong, C.-J. Wei, N. Van Hoeven, J. P. Gorres, M. Nason, H. Andersen, T. M. Tumpey, and G. J. Nabel. 2010. Comparative efficacy of hemagglutinin, nucleoprotein, and matrix 2 protein gene-based vaccination against H5N1 influenza in mouse and ferret. *PLoS ONE* 5: e9812.
37. Hashem, A., B. Jaentschke, C. Gravel, M. Tocchi, T. Doyle, M. Rosu-Myles, R. He, and X. Li. 2012. Subcutaneous immunization with recombinant adenovirus expressing influenza A nucleoprotein protects mice against lethal viral challenge. *Hum. Vaccin. Immunother.* 8: 425–430.
38. Flaman, A. S., C. Gravel, A. M. Hashem, M. Tocchi, and X. Li. 2011. The effect of interferon-α on the expression of cytochrome P450 3A4 in human hepatoma cells. *Toxicol. Appl. Pharmacol.* 253: 130–136.
39. Hauser, H., L. Shen, Q.-L. Gu, S. Krueger, and S.-Y. Chen. 2004. Secretory heat-shock protein as a dendritic cell-targeting molecule: a new strategy to enhance the potency of genetic vaccines. *Gene Ther.* 11: 924–932.
40. Gravel, C., C. Li, J. Wang, A. M. Hashem, B. Jaentschke, K.-W. Xu, B. Lorbetskie, G. Gingras, Y. Aubin, G. Van Domselaar, et al. 2010. Qualitative and quantitative analyses of virtually all subtypes of influenza A and B viral neuraminidases using antibodies targeting the universally conserved sequences. *Vaccine* 28: 5774–5784.
41. Walzl, G., S. Tafuro, P. Moss, P. J. Openshaw, and T. Hussell. 2000. Influenza virus lung infection protects from respiratory syncytial virus-induced immunopathology. *J. Exp. Med.* 192: 1317–1326.
42. Heer, A. K., A. Shamshiev, A. Donda, S. Uematsu, S. Akira, M. Kopf, and B. J. Marsland. 2007. TLR signaling fine-tunes anti-influenza B cell responses without regulating effector T cell responses. *J. Immunol.* 178: 2182–2191.
43. Commandeur, S., M. Y. Lin, K. E. van Meijgaarden, A. H. Friggen, K. L. M. C. Franken, J. W. Drijfhout, G. E. Korsvold, F. Oftung, A. Geluk, and T. H. M. Ottenhoff. 2011. Double- and monofunctional CD4$^+$ and CD8$^+$ T-cell responses to Mycobacterium tuberculosis DosR antigens and peptides in long-term latently infected individuals. *Eur. J. Immunol.* 41: 2925–2936.
44. Hashem, A. M., A. S. Flaman, A. Farnsworth, E. G. Brown, G. Van Domselaar, R. He, and X. Li. 2009. Aurintricarboxylic acid is a potent inhibitor of influenza A and B virus neuraminidases. *PLoS ONE* 4: e8350.
45. Prokudina, E. N., N. P. Semenova, V. M. Chumakov, I. A. Rudneva, and S. S. Yamnikova. 2001. Extracellular truncated influenza virus nucleoprotein. *Virus Res.* 77: 43–49.
46. Watanabe, H., K. Numata, T. Ito, K. Takagi, and A. Matsukawa. 2004. Innate immune response in Th1- and Th2-dominant mouse strains. *Shock* 22: 460–466.
47. Almeida, J. R., D. A. Price, L. Papagno, Z. A. Arkoub, D. Sauce, E. Bornstein, T. E. Asher, A. Samri, A. Schnuriger, I. Theodorou, et al. 2007. Superior control of HIV-1 replication by CD8+ T cells is reflected by their avidity, polyfunctionality, and clonal turnover. *J. Exp. Med.* 204: 2473–2485.
48. Darrah, P. A., D. T. Patel, P. M. De Luca, R. W. B. Lindsay, D. F. Davey, B. J. Flynn, S. T. Hoff, P. Andersen, S. G. Reed, S. L. Morris, et al. 2007. Multifunctional TH1 cells define a correlate of vaccine-mediated protection against *Leishmania major*. *Nat. Med.* 13: 843–850.
49. Kannanganat, S., C. Ibegbu, L. Chennareddi, H. L. Robinson, and R. R. Amara. 2007. Multiple-cytokine-producing antiviral CD4 T cells are functionally superior to single-cytokine-producing cells. *J. Virol.* 81: 8468–8476.
50. Adams, W. C., E. Bond, M. J. E. Havenga, L. Holterman, J. Goudsmit, G. B. Karlsson Hedestam, R. A. Koup, and K. Loré. 2009. Adenovirus serotype 5 infects human dendritic cells via a coxsackievirus-adenovirus receptor-independent receptor pathway mediated by lactoferrin and DC-SIGN. *J. Gen. Virol.* 90: 1600–1610.
51. Carragher, D. M., D. A. Kaminski, A. Moquin, L. Hartson, and T. D. Randall. 2008. A novel role for non-neutralizing antibodies against nucleoprotein in facilitating resistance to influenza virus. *J. Immunol.* 181: 4168–4176.
52. Yewdell, J. W., E. Frank, and W. Gerhard. 1981. Expression of influenza A virus internal antigens on the surface of infected P815 cells. *J. Immunol.* 126: 1814–1819.
53. Germann, T., M. Bongartz, H. Dlugonska, H. Hess, E. Schmitt, L. Kolbe, E. Kölsch, F. J. Podlaski, M. K. Gately, and E. Rüde. 1995. Interleukin-12 profoundly up-regulates the synthesis of antigen-specific complement-fixing IgG2a, IgG2b and IgG3 antibody subclasses in vivo. *Eur. J. Immunol.* 25: 823–829.
54. Brown, M. P., D. J. Topham, M. Y. Sangster, J. Zhao, K. J. Flynn, S. L. Surman, D. L. Woodland, P. C. Doherty, A. G. Farr, P. K. Pattengale, and M. K. Brenner. 1998. Thymic lymphoproliferative disease after successful correction of CD40 ligand deficiency by gene transfer in mice. *Nat. Med.* 4: 1253–1260.
55. Jain, A., J. A. Kovacs, D. L. Nelson, S. A. Migueles, S. Pittaluga, W. Fanslow, X. Fan, D. W. Wong, J. Massey, R. Hornung, et al. 2011. Partial immune reconstitution of X-linked hyper IgM syndrome with recombinant CD40 ligand. *Blood* 118: 3811–3817.
56. Chougnet, C. 2003. Role of CD40 ligand dysregulation in HIV-associated dysfunction of antigen-presenting cells. *J. Leukoc. Biol.* 74: 702–709.
57. Zhang, R., J. D. Lifson, and C. Chougnet. 2006. Failure of HIV-exposed CD4+ T cells to activate dendritic cells is reversed by restoration of CD40/CD154 interactions. *Blood* 107: 1989–1995.
58. Eaton, S. M., E. M. Burns, K. Kusser, T. D. Randall, and L. Haynes. 2004. Age-related defects in CD4 T cell cognate helper function lead to reductions in humoral responses. *J. Exp. Med.* 200: 1613–1622.
59. Malaspina, A., S. Moir, S. M. Orsega, J. Vasquez, N. J. Miller, E. T. Donoghue, S. Kottilil, M. Gezmu, D. Follmann, G. M. Vodeiko, et al. 2005. Compromised B cell responses to influenza vaccination in HIV-infected individuals. *J. Infect. Dis.* 191: 1442–1450.
60. Nabel, G. J., and A. S. Fauci. 2010. Induction of unnatural immunity: prospects for a broadly protective universal influenza vaccine. *Nat. Med.* 16: 1389–1391.
61. Steel, J., A. C. Lowen, T. T. Wang, M. Yondola, Q. Gao, K. Haye, A. García-Sastre, and P. Palese. 2010. Influenza virus vaccine based on the conserved hemagglutinin stalk domain. *MBio* 1: e00018–e10.
62. Breathnach, C. C., H. J. Clark, R. C. Clark, C. W. Olsen, H. G. Townsend, and D. P. Lunn. 2006. Immunization with recombinant modified vaccinia Ankara (rMVA) constructs encoding the HA or NP gene protects ponies from equine influenza virus challenge. *Vaccine* 24: 1180–1190.
63. Donnelly, J. J., A. Friedman, J. B. Ulmer, and M. A. Liu. 1997. Further protection against antigenic drift of influenza virus in a ferret model by DNA vaccination. *Vaccine* 15: 865–868.
64. Ulmer, J. B., T. M. Fu, R. R. Deck, A. Friedman, L. Guan, C. DeWitt, X. Liu, S. Wang, M. A. Liu, J. J. Donnelly, and M. J. Caulfield. 1998. Protective CD4+ and CD8+ T cells against influenza virus induced by vaccination with nucleoprotein DNA. *J. Virol.* 72: 5648–5653.
65. Roy, S., G. P. Kobinger, J. Lin, J. Figueredo, R. Calcedo, D. Kobasa, and J. M. Wilson. 2007. Partial protection against H5N1 influenza in mice with a single dose of a chimpanzee adenovirus vector expressing nucleoprotein. *Vaccine* 25: 6845–6851.